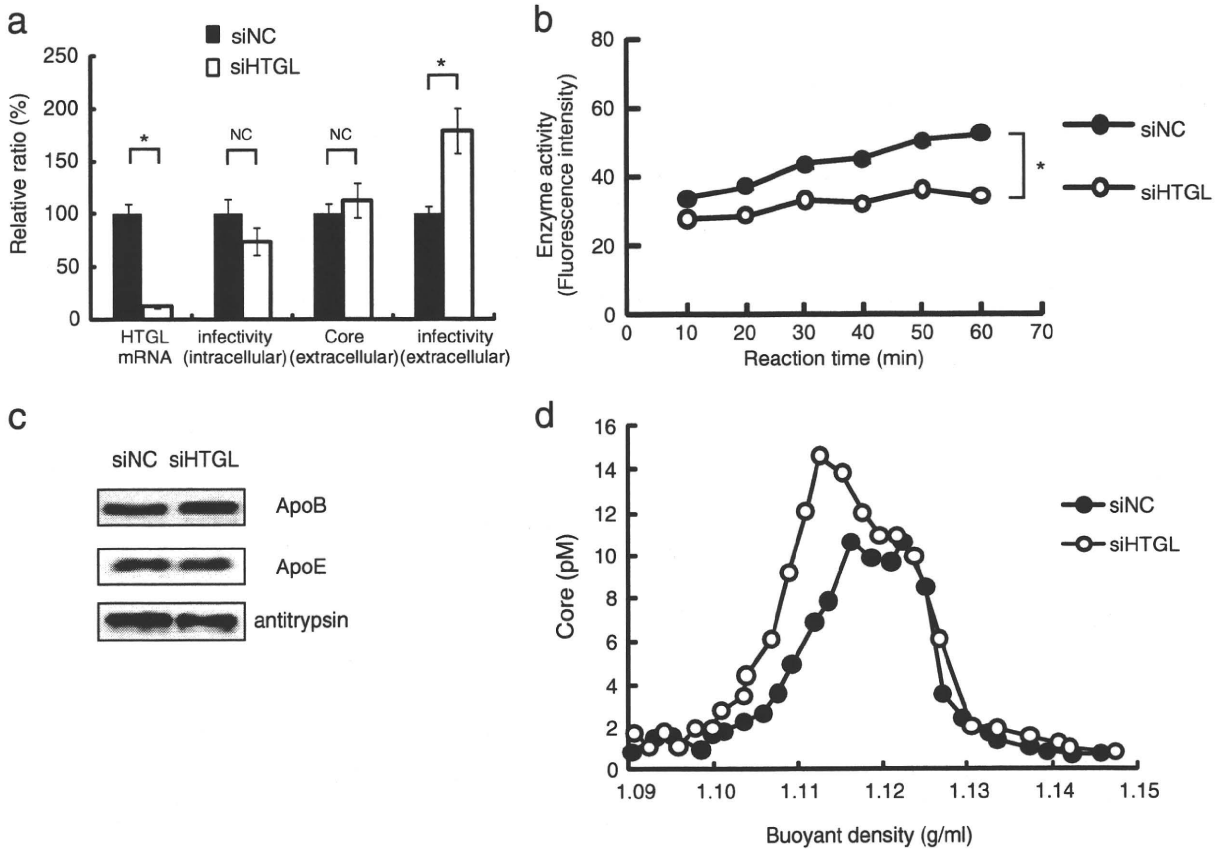

Fig. 4. HCV with higher infectivity and a lower buoyant density in the medium from HTGL knockdown cells. a. HTGL mRNA, infectivity of HCV within cells, extracellular Core and infectivity of HCV in the medium are shown. The mean percentages relative to control cells are shown with the standard deviation (mRNA, Core; n = 3, infectivity; n = 5). Statistically significant differences in HTGL mRNA level and extracellular infectivity are indicated by asterisks (Student's *t*-test): $*p<0.001$. There was no statistically significant difference in intracellular infectivity and extracellular core (Student's *t*-test): NS $p>0.01$. b. Activities of HTGL were determined. After secretion, most of the HTGL is bound to heparan sulfate proteoglycans (HSPG) at the cell surface (Connelly, 1999; S.-Fojo et al., 2004). Both HTGLs bound and unbound to HSPG are expected to act on lipoproteins in the medium. Thus, in order to evaluate activities of HTGL acting on lipoproteins in the medium, heparin (10 U/ml) was added to the medium to release HTGL bound to HSPG at 24 h post-transfection of siRNA. The medium was harvested at 48 h post-transfection, passed through 0.45 μm filter (Iwaki) to eliminate cell debris and used for the assay. Statistically significant difference in HTGL activity at 60 min is indicated by asterisks (Student's *t*-test): $*p<0.001$. c. Detection of apolipoproteins (ApoB and ApoE) and α-1 antitrypsin as standard secreted in culture medium from HTGL knockdown cells and control cells. d. Buoyant density of HCV produced from HTGL knockdown cells. The HCV-bearing medium from HTGL knockdown cells was subjected to centrifugation in an iodixanol gradient. After ultracentrifugation, aliquots of 80 consecutive fractions were collected and analyzed for Core by ELISA. The data are presented from 25 fractions around Core peak from a single representative experiment of three experiments. There was a significant difference in the buoyant density of the Core peak between HTGL knockdown cells and the control (Student's *t*-test, $p<0.001$).

heparin leads to a release of LPL bound to HSPG (Kern et al., 1990). Therefore, it is conceivable that HCV infectivity could be reduced through activities of LPL in the circulation at a lesser efficiency than observed in this work. Here, we demonstrated that the hydrolyzing activity of HTGL as well as LPL affects HCV infectivity. Considering this lipase-induced reduction in HCV infectivity in the circulation, it is important for virus to infect the proximal hepatocytes before entering circulation. In other words, the activities of LPL and/or HTGL may be one host mechanism to resist invasion and spread of HCV.

Materials and methods

Cell culture

HuH7.5, HeLa, 293T and HepG2 cells were maintained in DMEM supplemented with 10% FBS, 100 U/ml penicillin and 100 μg/ml streptomycin.

Virus source

HuH7.5 cells were transfected with HCV 2a strain, JFH1 RNA genome and maintained in DMEM supplemented with 10% FBS, 100 U/ml penicillin and 100 μg/ml streptomycin. Three days before harvest, medium was replaced with Opti-Pro (Invitrogen) supplemented with 0.1% BSA. Culture medium was filtered with 0.45 μm filter (Iwaki) and used as virus source (the HCV-bearing medium).

HCV infectivity

To determine HCV infectivity in the medium, HuH7.5 cells were inoculated with the HCV-bearing medium (MOI of 0.5) at 37 °C for 2 h. Cells were washed with PBS and incubated in DMEM supplemented with 10% FBS, 100 U/ml penicillin and 100 μg/ml streptomycin. Cells were fixed at 24 h post-inoculation and subjected to immunofluorescence staining using serum from a HCV-positive individual to detect HCV-infected cells. Three to five fields under microscope were randomly selected. Cells in a field were counted and the percentage of HCV-positive cells to total cells (around 500–1000) was calculated.

To determine HCV infectivity within cells, cells were collected by trypsinization. After washing with PBS, cells were incubated with water and passed through a 27-gauge needle (Terumo) at ten times. After centrifugation, supernatant was passed through a 0.45 μm filter (Iwaki) and inoculated to HuH7.5 cells. Immunofluorescence staining was performed as mentioned above.

Lipase activity

Total lipase test (Progen) and hepatic lipase select test (Progen) were used to examine LPL activity and HTGL activity, respectively, according to the manufacturer's protocol.

Iodixanol density gradients

The HCV-bearing medium was concentrated around 50 times using amicon ultra-15 100k (Millipore) and treated with PBS or 5, 50, or 500 μg/ml of LPL at 37 °C for 1 h. The samples were applied to the top of a linear gradient formed from 17–37% iodixanol-containing PBS and spun at 36,000 rpm for 18 h at 4 °C using a SRP 41 Hitachi Ultracentrifuge rotor. Aliquots of 30 consecutive fractions were collected and used for analyses of Core, infectivity, HCV RNA, and immunoprecipitation with anti-ApoB or anti-ApoE antibodies.

For analysis of the HCV-bearing medium from HTGL knockdown cells, the concentrated samples were applied to the top of a gradient from 14–54% iodixanol-containing PBS and spun at 34,000 rpm for 20 h at 4 °C. A total of 80 consecutive fractions were collected and used for analyses of Core.

Quantification of HCV RNA

RNA was extracted from fractions of the iodixanol gradient using an RNeasy mini kit (Qiagen). Complementary DNA was prepared by incubating RNA with SuperScript III (Invitrogen) and 737R primer, a reverse RNA primer of HCV genome (Sugiyama et al., 2009). Quantitative PCR analysis was performed by 7500 Fast Real Time PCR System (Applied Biosystems). Taqman probe and primers were as follows: probe 733FB (Sugiyama et al., 2009), forward 5′-CCCTCCCGGGAGAGCCATAGTG-3′, reverse 5′-GTCTCGCGGGGGCACGCCCAAAT-3′. The copy number of HCV was determined by the standard-curve method with serial dilutions of the synthesized full-length HCV RNA.

Immunoprecipitation

Fractions from iodixanol gradient were incubated with anti-ApoB antibody (Biodesign International) or anti-ApoE antibody (Chemicon International) for 2 h at room temperature. Protein G sepharose (GE) was added and the immunocomplex was collected by centrifugation. The pellets were used for RNA extraction.

Expression of LPL and HTGL

RNA was extracted from cells using RNeasy mini kit (Qiagen). Complementary DNA was prepared by incubating RNA with Super-Script III (Invitrogen) and oligo(dT) as an universal primer. Quantitative PCR analysis was performed with primers specific for LPL (Lindegaard et al., 2005), for HTGL (Sirvent et al., 2004), and for GAPDH (Suzuki et al., 2008). The LPL and HTGL mRNA expression level was calibrated with the level of GAPDH mRNA expression.

Neutralization of HTGL

The HCV-bearing medium was incubated with IgG rabbit (Santa Cruz) or anti-HTGL antibody (sc-21007, Santa Cruz) at 4 °C overnight, followed by PBS or LPL treatment at 37 °C for 1 h. HuH7.5 cells were inoculated with the medium at 37 °C for 2 h and subjected to immunofluorescence staining as explained above.

Knockdown of HTGL

siRNA (siGENOME SMART pool M-008743-00-0005, Thermo) at a final concentration of 40 nM was transfected with HuH7.5 cells using siLentFect reagent (Bio-Rad). The HCV-bearing medium (MOI = 0.5) was inoculated with cells at 4 h post-transfection. Then, fresh medium was replaced 2 h later. At 24 h post-transfection, medium was replaced with Opti-pro (Invitrogen) supplemented with 0.1% BSA. At 48 h post-transfection, culture medium and cells were used for analyses of RNA, infectivity, Western blotting and buoyant density.

Western blotting

Western blotting was performed using anti-ApoB antibody (Biodesign International), anti-ApoE antibody (Innogenetics) and anti-α-1 antitrypsin antibody (Biodesign). Detection was carried out using ECL plus reagent (GE).

Supplementary materials related to this article can be found online at doi:10.1016/j.virol.2010.08.011.

Acknowledgments

We are grateful to Drs. T. Wakita and C. Rice for their kind gifts of JFH1 and HuH7.5 cells, respectively. We thank H. Kato, R. Shiina, E. Sugawara, R. Tobita, and H. Yamamoto (Chiba Institute of Technology) for their technical assistance. This study was supported by Grants-in-Aid for Scientific Research from the Ministry of Health, Labor, and Welfare of Japan and from the Ministry of Education, Culture, Sports, Science, and Technology.

References

André, P., K.-Pradel, F., Deforges, S., Perret, M., Berland, J.L., Sodoyer, M., Pol, S., Bréchot, C., P.-Baccalà, G., Lotteau, V., 2002. Characterization of low- and very-low-density hepatitis C virus RNA-containing particles. J. Virol. 76, 6919–6928.

Andréo, U., Maillard, P., Kalinina, O., Walic, M., Meurs, E., Martinot, M., Marcellin, P., Budkowska, A., 2007. Lipoprotein lipase mediates hepatitis C virus (HCV) cell entry and inhibit HCV infection. Cell. Microbiol. 9, 2445–2456.

Braun, J.E.A., Severson, D.L., 1992. Regulation of the synthesis, processing and translocation of lipoprotein lipase. Biochem. J. 287, 337–347.

Chang, K.-S., Jiang, J., Cai, Z., Luo, G., 2007. Human apolipoprotien E is required for infectivity and production of hepatitis C virus in cell culture. J. Virol. 81, 13783–13793.

Connelly, P.W., 1999. The role of hepatic lipase in lipoprotein metabolism. Clin. Chim. Acta 286, 243–255.

Gastaminza, P., Cheng, G., Wieland, S., Zhong, J., Liao, W., Chisari, F.V., 2008. Cellular determinants of hepatitis C virus assembly, maturation, degradation, and secretion. J. Viol. 82, 2120–2129.

Huang, H., Son, F., Owen, D.M., Li, W., Chen, Y., Gale Jr., M., Ye, J., 2007. Hepatits C virus production by human hepatocytes dependent on assembly and secretion of very low-density lipoprotein. Proc. Natl Acad. Sci. 104, 5848–5853.

Icard, V., Diaz, O., Scholtes, C., P.-Cocon, L., Ramière, C., Bartenschlager, R., Penin, F., Lotteau, V., André, P., 2009. Secretion of hepatitis C virus envelope glycoproteins depends on assembly of apolipoprotein B positive lipoproteins. PLoS ONE 4, e4233.

Jiang, J., Luo, G., 2009. Apolipoprotein E but not B is required for the formation of infectious hepatitis C virus particles. J. Virol. 83, 12680–12691.

Kern, P.A., Martin, R.A., Carty, J., Goldberg, I.J., Ong, J.M., 1990. Identification of lipoprotein lipase immunoreactive protein in pre- and posthepain plasma from normal subjects and patients with type I hyperlipoproteinemia. J. Lipid Res. 31, 17–26.

Lindegaard, M.L.S., Olivecrona, G., Christoffersen, C., Kratky, D., Hannibal, J., Petersen, B.L., Zechner, R., Damm, P., Nielsen, L.B., 2005. Endothelial and lipoprotein lipases in human and mouse placenta. J. Lipid Res. 46, 2339–2346.

Mead, J.L., Irvine, S.A., Ramji, D.P., 2002. Lipoprotein lipase: structure, function, regulation, and role in disease. J. Mol. Med. 80, 753–769.

Olofsson, S.-O., Borèn, J., 2005. Apolipoprotein B: a clinically important apolipoprotein which assembles atherogenic lipoproteins and promotes the development of atherosclerosis. J. Intern. Med. 258, 395–410.

Owen, D.M., Huang, H., Ye, J., Gale Jr., M., 2009. Apolipoprotein E on hepatitis C virion facilitates infection through interaction with low-density lipoprotein receptor. Virology 394, 99–108.

S.-Fojo, S., G.-Navarro, H., Freeman, L., Wagner, E., Nong, Z., 2004. Hepatic lipase, lipoprotein metabolism, and atherogenesis. Arterioscler. Thromb. Vasc. Biol. 24, 1750–1754.

Sirvent, A., Verhoeven, A.J.M., Jansen, H., Kosykh, V., Darteil, R.J., Hum, D.W., Fruchart, J.-C., Staels, B., 2004. Farnesoid X receptor represses hepatic lipase gene expression. J. Lipid Res. 45, 2110–2115.

Sugiyama, K., Suzuki, K., Nakazawa, T., Funami, K., Hishiki, T., Ogawa, K., Saito, S., Shimotohno, K.W., Suzuki, T., Shimizu, Y., Tobiba, R., Hijikata, M., Takaku, H., Shimotohno, K., 2009. Genetic analysis of Hepatitis C virus with defective genome and its infectivity in vitro. J. Virol. 83, 6922–6928.

Suzuki, K., Nakamura, K., Iwata, Y., Sekine, Y., Kawai, M., Sugihara, G., Tsuchiya, K.J., Suda, S., Matsuzaki, H., Takei, N., Hashimoto, K., Mori, N., 2008. Decreased

expression of reelin receptor VLDLR in peripheral lymphocytes of drug-naïve schizophrenic patients. Schizophrenia Res. 98, 148–156.
Thomssen, R., Bonk, S., Propfe, C., Heermann, K.-H., Köchel, H.G., Uy, A., 1992. Association of hepatitis C virus in human sera with b-lipoprotein. Med. Microbiol. Immunol. 181, 293–300.
Thomssen, R., Bonk, S., Thiele, A., 1993. Density heterogeneities of hepatitis C virus in human sera due to the binding of β-lipoproteins and immunoglobulins. Med. Microbiol. Immunol. 182, 329–334.
Thomssen, R., Bonk, S., 2002. Virolytic action of lipoprotein lipase on hepatitis C virus in human sera. Med. Microbiol. Immunol. 191, 17–24.

JOURNAL OF VIROLOGY, Nov. 2010, p. 11761–11770 Vol. 84, No. 22
0022-538X/10/$12.00 doi:10.1128/JVI.00638-10

Sphingomyelin Activates Hepatitis C Virus RNA Polymerase in a Genotype-Specific Manner▽†

Leiyun Weng,[1] Yuichi Hirata,[2] Masaaki Arai,[3] Michinori Kohara,[2] Takaji Wakita,[4] Koichi Watashi,[4,5] Kunitada Shimotohno,[5,6] Ying He,[7] Jin Zhong,[7] and Tetsuya Toyoda[1]*

Units of Viral Genome Regulation[1] and Viral Hepatitis,[7] Institut Pasteur of Shanghai, Key Laboratory of Molecular Virology and Immunology, Chinese Academy of Sciences, 411 Hefei Road, 200025 Shanghai, People's Republic of China; Department of Microbiology and Cell Biology, Tokyo Metropolitan Institute of Medical Biology, 3-18-22 Honkomagome, Bunkyo-Ku, Tokyo 113-8613, Japan[2]; Pharmacology Laboratory, Pharmacology Department V, Mitsubishi Tanabe Pharma Corporation, 1000 Kamoshida-cho, Aoba-ku, Yokohama 227-0033, Japan[3]; Department of Virology II, National Institute of Health, 1-23-1 Toyama, Shinjuku, Tokyo 132-8640, Japan[4]; Laboratory of Human Tumor Viruses, Department of Viral Oncology, Institute for Virus Research, Kyoto University, Kyoto 606-8507, Japan[5]; and Chiba Institute of Technology, 2-17-1 Tsudamuna, Narashino, Chiba 275-0016, Japan[6]

Received 25 March 2010/Accepted 27 August 2010

Hepatitis C virus (HCV) replication and infection depend on the lipid components of the cell, and replication is inhibited by inhibitors of sphingomyelin biosynthesis. We found that sphingomyelin bound to and activated genotype 1b RNA-dependent RNA polymerase (RdRp) by enhancing its template binding activity. Sphingomyelin also bound to 1a and JFH1 (genotype 2a) RdRps but did not activate them. Sphingomyelin did not bind to or activate J6CF (2a) RdRp. The sphingomyelin binding domain (SBD) of HCV RdRp was mapped to the helix-turn-helix structure (residues 231 to 260), which was essential for sphingomyelin binding and activation. Helix structures (residues 231 to 241 and 247 to 260) are important for RdRp activation, and 238S and 248E are important for maintaining the helix structures for template binding and RdRp activation by sphingomyelin. 241Q in helix 1 and the negatively charged 244D at the apex of the turn are important for sphingomyelin binding. Both amino acids are on the surface of the RdRp molecule. The polarity of the phosphocholine of sphingomyelin is important for HCV RdRp activation. However, phosphocholine did not activate RdRp. Twenty sphingomyelin molecules activated one RdRp molecule. The biochemical effect of sphingomyelin on HCV RdRp activity was virologically confirmed by the HCV replicon system. We also found that the SBD was the lipid raft membrane localization domain of HCV NS5B because JFH1 (2a) replicon cells harboring NS5B with the mutation A242C/S244D moved to the lipid raft while the wild type did not localize there. This agreed with the myriocin sensitivity of the mutant replicon. This sphingomyelin interaction is a target for HCV infection because most HCV RdRps have 241Q.

Hepatitis C virus (HCV) has a positive-stranded RNA genome and belongs to the family *Flaviviridae* (21). HCV chronically infects more than 130 million people worldwide (34), and HCV infection often induces liver cirrhosis and hepatocellular carcinoma (19, 28). To date, pegylated interferon (PEG-IFN) and ribavirin are the standard treatments for HCV infection. However, many patients cannot tolerate their serious side effects. Therefore, the development of new and safer therapeutic methods with better efficacy is urgently needed.

Lipids play important roles in HCV infection and replication. For example, the HCV core associates with lipid droplets and recruits nonstructural proteins and replication complexes to lipid droplet-associated membranes which are involved in the production of infectious virus particles (24). HCV RNA replication depends on viral protein association with raft membranes (2, 30). The association of cholesterol and sphingolipid with HCV particles is also important for virion maturation and infectivity (3). The inhibitors of the sphingolipid biosynthetic pathway, ISP-1 and HPA-12, which specifically inhibit serine palmitoyltransferase (SPT) (23) and ceramide trafficking from the endoplasmic reticulum (ER) to the Golgi apparatus (37), suppress HCV virus production in cell culture but not viral RNA replication by the JFH1 replicon (3). Other serine SPT inhibitors (myriocin and NA255) inhibit genotype 1b replication (4, 29, 33). Very-low-density lipoprotein (VLDL) also interacts with the HCV virion (15).

Sakamoto et al. reported that sphingomyelin bound to HCV RNA-dependent polymerase (RdRp) at the sphingomyelin binding domain (SBD; amino acids 230 to 263 of RdRp) to recruit HCV RdRp on the lipid rafts, where the HCV complex assembles, and that NA255 suppressed HCV replication by releasing HCV RdRp from the lipid rafts (29). In the present study, we analyzed the effect of sphingomyelin on HCV RdRp activity *in vitro* and found that sphingomyelin activated HCV RdRp activity in a genotype-specific manner. We also determined the sphingomyelin activation domain and the activation mechanism. Finally, we confirmed our biochemical data by a HCV replicon system.

* Corresponding author. Mailing address: Unit of Viral Genome Regulation, Institut Pasteur of Shanghai, Chinese Academy of Sciences, 411 Hefei Road, 200025 Shanghai, People's Republic of China. Phone and fax: 86 21 6385 1621. E-mail: ttoyoda@amber.plala.or.jp.

† Supplemental material for this article may be found at http://jvi.asm.org.

▽ Published ahead of print on 15 September 2010.

MATERIALS AND METHODS

HCV RNA polymerase. A C-terminal 21-amino-acid deletion was made to the HCV RdRps of strains HCR6 (genotype 1b) (36), NN (1b) (35), Con1 (1b) (5), JFH1 (2a) (36), J6CF (2a) (25), H77 (1a) (7), and RMT (1a), and the mutants

were purified from bacteria as described previously (36). HCR6 (1b) RdRp with the mutation L245A [RdRp(L245A)] or I253A [RdRp(I253A)] or the double mutation L245A and I253A [RdRp(L245A/I253A)]; JFH1 (2a) RdRp with the mutation(s) A242C/S244D, A242, S244D, or T251Q; J6CF (2a) RdRp with the mutation(s) R241Q, S244D, or R241Q/S244D; and H77 (1a) RdRp(A238S/Q248E) were introduced using an *in vitro* mutagenesis kit (Stratagene) and the oligonucleotides listed in Table S1 in the supplemental material. HCR6 (1b) His_6-tagged RdRp(L245A/I253A) was removed from pET21b/KM (36) and cloned into the BamHI/XhoI site of pGEX-6P-3 (GE), resulting in pGEXHCVHCR6RdRp(L245A/I253A).

***In vitro* HCV transcription.** *In vitro* HCV transcription was performed as described previously (36). Briefly, following 30 min of preincubation without ATP, CTP, or UTP, 100 nM HCV RdRp was incubated in 50 mM Tris-HCl (pH 8.0), 200 mM monopotassium glutamate, 3.5 mM $MnCl_2$, 1 mM dithiothreitol (DTT), 0.5 mM GTP, 50 μM ATP, 50 μM CTP, 5 μM [α-^{32}P]UTP, 200 nM RNA template (SL12-1S), 100 U/ml human placental RNase inhibitor, and the lipid (amount indicated below) at 29°C for 90 min. ^{32}P-labeled RNA products were subjected to 6% polyacrylamide gel electrophoresis (PAGE) containing 8 M urea. The resulting autoradiograph was analyzed with a Typhoon Trio plus image analyzer (GE).

RNA filter binding assay. An RNA filter binding assay was performed as described previously (36). Briefly, 100 nM HCV RdRp and 100 nM ^{32}P-labeled RNA template (SL12-1S) were incubated with or without 0.01 mg/ml egg yolk sphingomyelin in 25 μl of 50 mM Tris-HCl (pH 7.5), 200 mM monopotassium glutamate, 3.5 mM $MnCl_2$, and 1 mM DTT at 29°C for 30 min. After incubation, the solutions were diluted with 0.5 ml of TE (50 mM Tris-HCl [pH 7.5], 1 mM EDTA) buffer and filtered through nitrocellulose membranes (0.45-μm pore size; Millipore). The filter was washed five times with TE buffer, and the bound radioisotope was analyzed by Typhoon Trio plus after being dried.

Enzyme-linked immunosorbent assay (ELISA). Ninety-six-well microtiter plates (Corning) were coated with 250 ng of egg yolk sphingomyelin in ethanol by evaporation at room temperature. After the wells were blocked with phosphate-buffered saline (PBS) and 3% bovine serum albumin (BSA), they were incubated with 1 pmol of the HCV RdRp of HCR6 (1b) wild type (wt) or L245A, I253A, or L245A/I253A mutant; NN (1b); H77 (1a); RMT (1a); J6CF (2a); or JFH1 (2a) wt or A242C/S244D, A242, S244D, or T251Q mutant in Tris-buffered saline (50 mM Tris-HCl [pH 7.5] and 150 mM NaCl) for 1.5 h at room temperature. After being blocked with 3% BSA, the bound HCV RdRp was detected by adding rabbit anti-HCV RdRp serum (1:5,000) (see Fig. S1 in the supplemental material) (17) before incubation with a horseradish peroxidase (HRP)-conjugated anti-rabbit IgG antibody (1:5,000; Southern Biotech). The optical density at 450 nm (OD_{450}) was measured with a Spectra Max 190 spectrophotometer (Molecular Devices) using a TMB (3,3′,5,5′-tetramethylbenzidine) Liquid Substrate System (Sigma).

HCV subgenomic replicon. A D244S mutation was introduced into the HCV strain NN (1b) subgenomic replicon pLMH14 (35), resulting in pLMH(NN)5B(D244S) [where 5B(D244S) is the NS5B protein with the mutation D244S]. The A242C/S244D mutation was introduced into the HCV JFH1 (2a) replicon, pSGR-JFH1/luc (25), resulting in pSGR-JFH1/luc5B(A242C/S244D). The HpaI and XbaI fragment of pSGR-JFH1 (18) was replaced with that of pSGR-JFH1/luc5B(A242C/S244D), resulting in pSGR-JFH15B(A242C/S244D). The A238S/Q248E mutation was introduced into HCV H77 (1a) replicon pHCVrep13(S2204I)/Neo (7) after the neomycin gene was replaced by the firefly luciferase gene [pH77(I)/luc] by insertion of AflII and AscI sites (see Table S1 in the supplemental material), resulting in pH77(I)/luc5B(A238S/Q248E). Subgenomic replicon RNA was transcribed *in vitro* by T7 RNA polymerase using MegaScript (Ambion) after the replicon plasmids were linearized by XbaI (strain NN and JFH1 replicons) or HpaI (strain H77 replicon). Subgenomic replicon RNA was stored at −80°C after being purified by phenol-chloroform extraction and ethanol precipitation.

Replicon assay with myriocin. Huh7.5.1 cells were kindly provided by F. Chisari and were maintained in Dulbecco's modified Eagle's medium (DMEM; Gibco) with 10% fetal bovine serum (FBS; Gibco) (38). HCV replicon RNA (10 μg) was transfected into 4×10^6 Huh7.5.1 cells (1×10^7/ml) in OptiMEM I (Gibco) by electroporation (GenePulser Xcell; Bio-Rad) at 270 V, 100 Ω, and 950 μF. After transfection, the cells were plated in 12-well plates incubated in DMEM–10% FBS. At 6 h after transfection, cells were treated with 0, 5, and 50 nM myriocin. At 4, 54, and 78 h after transfection (48 and 72 h after myriocin treatment), the cells were harvested, and luciferase activity was measured using a Dual-Glo luciferase assay kit and a GloMax 96 Microplate Luminometer (Promega). Luciferase activity was normalized against the activity at 4 h after transfection (26).

HCV JFH1 wt and NS5B(A242C/S244D) replicon cells. Huh7/scr cells were kindly provided by F. Chisari of the Scripps Research Institute and were maintained in Dulbecco's modified Eagle's medium (Gibco) with 10% fetal bovine serum (Gibco). RNA (10 μg each) from SGR-JFH1 and SGR-JFH1 with the mutations A242C/S244D in NS5B [NS5B(A242C/S244D) was transfected into 4×10^6 Huh7/scr cells (1×10^7/ml) in OptiMEM I (GIBCO) by electroporation (GenePulser Xcell; Bio-Rad) at 270 V, 100 Ω, and 950 μF. After transfection, the cells were plated in 10-cm dishes and incubated in DMEM–10% FBS with 1.0 and 0.5 mg/ml G418 (Gibco). JFH1 wt and NS5B(A242C/S244D) replicon cells were maintained in DMEM–10% FBS and 0.5 mg/ml G418.

Membrane floating assay. JFH1 wt and NS5B(A242C/S244D) replicon cells were suspended in two packed cell volumes of hypotonic buffer (10 mM HEPES-NaOH [pH 7.6], 10 mM KCl, 1.5 mM $MgCl_2$, 2 mM DTT, and 1 tablet/25 ml of EDTA-free protease inhibitor cocktail tablets [Roche]) and disrupted by 30 strokes of homogenization in a Dounce homogenizer using a tight-fitting pestle at 4°C. After nuclei were removed by centrifugation at 2,000 rpm for 10 min at 4°C, the supernatant (postnuclear supernatant [PNS]) was treated with 1% Triton X-100 in TNE buffer (25 mM Tris-HCl [pH 7.6] 150 mM NaCl, 1 mM EDTA) for 30 min on ice. The lysates were supplemented with 40% sucrose and centrifuged at 38,000 rpm in a Beckman SW41 Ti rotor (Beckman Coulter) overlaid with 30% and 10% sucrose in TNE buffer at 4°C for 14 h.

Western blotting. Western blotting using anti-HCV RdRp (17), rabbit anti-NS3 (32), anti-NS5A (16) and anti-caveolin-2 was performed as previously published (17).

Reagent. Egg yolk sphingomyelin, cholesterol phosphocholine, myriocin, and rabbit anti-caveolin-2 antibodies were purchased from Sigma. Hexanoyl sphingomyelin, C_6-ceramide, C_8-β-D-glucosyl ceramide, and C_8-β-D-lactosyl ceramide were purchased from Avanti Polar Lipids. [α-^{32}P]UTP was purchased from New England Nuclear.

Statistical analysis. Significant differences were evaluated using *P* values calculated from a Student's *t* test.

Nucleotide sequence accession number. The sequence of HCV RMT has been deposited in the GenBank under accession number AB520610.

RESULTS

Sphingomyelin activation of HCV RNA polymerases of various genotypes. There are several sequence variations in the sphingomyelin binding domain (SBD; amino acids 231 to 260 of HCV RdRp) among HCV genotypes (see Fig. 7A). In order to compare the RdRps of different genotypes of HCV, we purified RdRp from genotypes 1b (strains HCR6, NN, and Con1), 1a (H77 and MRT), and 2a (JFH1 and J6CF) (see Fig. S2 in the supplemental material). First, the effect of ethanol on HCV HCR6 (1b) RdRp transcription was examined because lipids were suspended in ethanol before they were added to the HCV transcription reaction mixture. We found that 2% ethanol did not inhibit HCV transcription (see Fig. S3 in the supplemental material); therefore, all subsequent experiments were performed using less than 2% ethanol.

The kinetics of sphingomyelin activation were analyzed using egg yolk sphingomyelin for HCR6 (1b) RdRp wt (Fig. 1A) and subtype 2a (JFH1 and J6CF) RdRps (Fig. 1B), and *N*-hexanoyl-D-*erythro*-sphingosylphosphorylcholine (hexanoyl sphingomyelin) was used for HCR6 (1b) RdRp wt (Fig. 1C) and subtype 1a (H77 and RMT) RdRps (Fig. 1D). The egg yolk sphingomyelin activation curve of HCR6 (1b) RdRp wt at low concentrations (<0.01 mg/ml) was sigmoid. The transcription activity of HCR6 (1b) RdRp wt increased in a dose-dependent manner. It was activated 11-fold at 0.01 mg/ml and then plateaued (14-fold activation) at 0.1 mg/ml. However, JFH1 (2a) and J6CF (2a) RdRps were activated 2.5-fold and 2.2-fold, respectively, at 0.01 mg/ml sphingomyelin, at which point they plateaued.

Egg yolk sphingomyelin is a mixture. In order to obtain the optimal molar ratio for sphingomyelin activation of HCR6 (1b)

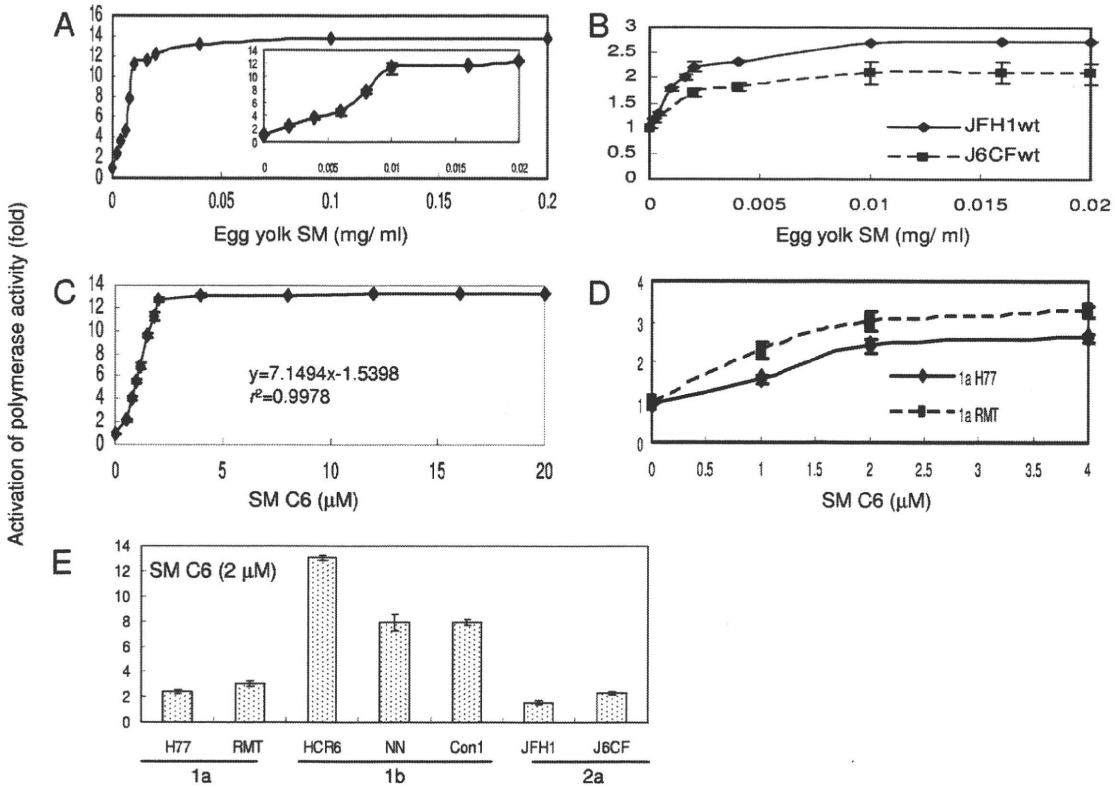

FIG. 1. Sphingomyelin activation of HCV RNA polymerases. (A) Activation kinetics of HCV HCR6 (1b) RdRp wt by egg yolk sphingomyelin (SM). The inset shows activation produced by 0 to 0.02 mg/ml egg yolk sphingomyelin. Activation kinetics of HCV 2a (JFH1 and J6CF) RdRps by egg yolk sphingomyelin (B) and of HCV HCR6 (1b) RdRp wt by hexanoyl sphingomyelin (SM C6) (C). In panel C, the first order of the graph was fitted by linear regression; the calculated equation is indicated in the graph. (D) Activation kinetics of HCV 1a (H77 and RMT) RdRps by hexanoyl sphingomyelin. (E) Activation effect of hexanoyl sphingomyelin on HCV RdRp of various genotypes. HCV RdRp (100 nM) was incubated with or without 2 μM SM C6. The names of the RdRps are indicated below the graph. Mean ± standard deviation of the activation ratio was calculated from three independent experiments.

RdRp wt, its activation kinetics were calculated using hexanoyl sphingomyelin (Fig. 1C, SM C6). The equation for the first-order ratio of hexanoyl sphingomyelin activation according to linear regression fitting was as follows: $y = 7.1494x - 1.5398$, where y is the activation ratio and x is the sphingomyelin concentration ($r^2 = 0.9978$). RdRp activation had almost plateaued at 2 μM hexanoyl sphingomyelin. The activation kinetics of JFH1 (2a) and J6CF (2a) RdRps in egg yolk sphingomyelin were biphasic and plateaued at 0.01 mg/ml. Those of RMT (1a) and H77 (1a) RdRps in hexanoyl sphingomyelin were also biphasic and plateaued at 2 μM. The curve of the first order was fitted by linear regression. The molar ratio of RdRp to hexanoyl sphingomyelin at its plateau was calculated as 1:20.

Because RdRp activation had almost plateaued at 2 μM hexanoyl sphingomyelin, we compared the effect of sphingomyelin on 100 M concentrations of RNA polymerases of the HCV 1a, 1b, and 2a genotypes using 2 μM hexanoyl sphingomyelin (Fig. 1E and Table 1).

Helix-turn-helix structure for sphingomyelin binding and activation. Sphingomyelin binds to the SBD peptide (see HCV SBD in Fig. 7) (29). Initially, we tested whether SBD was the sphingomyelin binding site in HCV RdRp by ELISA (Fig. 2A and Table 1). When the L245 and I253 residues of the SBD peptide were mutated to A, sphingomyelin binding activity was lost (29). We introduced the same mutations in HCV HCR6 (1b) RdRp and purified HCR6 (1b) RdRp with mutations L245A, I253A, and L245A/I253A. Because the C-terminal His-tagged HCR6 RdRp(L245A/I253A) was not soluble, it was solubilized by tagging of glutathione *S*-transferase (GST) sequence at the N terminus but lost polymerase activity. As the L245A/I253A mutant had lost its polymerase activity, polymerase activation was tested only for L245A and I253A (Fig. 2B and Table 1). These results confirmed that SBD located in the finger domain (residues 230E to 263G) successfully achieved sphingomyelin binding in HCV RdRp and that sphingomyelin did not bind to the SBD when the helix-turn-helix structure had been destroyed by the L245A or I253A mutation (29).

The sphingomyelin binding activities of genotype 1a and 2a RdRps were also tested (Fig. 2 and Table 1). Both JFH1 and J6CF were tested for genotype 2a because J6CF (2a) RdRp had an additional amino acid difference at position 241 in the SBD, and its sphingomyelin binding activity was very low (Fig. 2A and 7A; Table 1). J6CF (2a) RdRp(R241Q) showed the same sphingomyelin binding activity as HCR6 (1b) RdRp wt, indicating that 241Q was the critical amino acid for sphingomyelin binding. J6CF (2a) RdRp(S244D) and RdRp(R241Q/S244D) also showed higher sphingomyelin binding activity

TABLE 1. Summary of sphingomyelin activation of HCV RNA polymerase activities

Parameter	Value for the parameter by RdRp genotype, strain, and variant[a]																				
	1b							1a				2a									
	HCR6						RMT	H77		J6CF					JFH1					
	wt	L245A	I253A	L245A/I253A	D244S	NN	Con1	wt	wt	A238S/Q248E	wt	R241Q	S244D	R241Q/S244D	wt	A242C	S244D	A242C/S244D	T251Q
SM binding (%)[b]	100	24.3	30.8	15.5	78.7	93.4	117	144	86.7	82.5	19.3	118	53.1	80.2	70.4	75.5	93.1	92.4	80.7
Activation of polymerase (*n*-fold)[c]	13.0 (11.2)[d]	(2.8)[d]	(2.5)[d]	ND	3.6	7.9	7.9	3.0	2.0	8.1	2.3	4.3	5.6	3.4	1.6	1.0	3.1	4.4	1.8
Activation of RNA binding (*n*-fold)[c]	4.5	2.6	1.7	ND	1.9	ND	ND	ND	1.4	3.3	1.5	3.6	3.2	1.7	1.3	ND	ND	1.4	ND

[a] Numbers were averaged from three independent experiments. ND, not done.
[b] Egg yolk sphingomyelin (SM; 250 ng) was used.
[c] Hexanoyl sphingomyelin (2 μM) was used.
[d] Egg yolk sphingomyelin (0.01 mg/ml) was used.

than the wt ($P < 0.001$) but lower binding than the R241Q mutant. However, S244D showed higher RdRp activation than R241Q ($P < 0.005$), while the RdRp activation ratio of the double mutant (R241Q/S244D) was lower than that of S244D or R241Q, although all of them activated RdRp with sphingomyelin ($P < 0.005$) (Fig. 2A and C and Table 1). For JFH1, when the JFH1 RdRp SBD was modified (A242C/S244D) to allow it to bind with more sphingomyelin than the wt ($P < 0.005$), the mutant JFH1 RdRp(A242C/S244D) was activated more than the wt by sphingomyelin ($P < 0.005$) (Fig. 2A and C; Table 1). The sphingomyelin binding activity of JFH1 RdRp(T251Q) was 80.7% of that of HCR6 (1b), and its activation ratio was 1.8-fold. These results agree that SBD is both the sphingomyelin activation and binding domain and that the domains for these two activities are somehow different.

We determined which amino acid, 242C or 244D, enhanced sphingomyelin binding by comparing HCR6 (1b) and JFH1 (2a) RdRps. Sphingomyelin binding of HCR6 (1b) RdRp(D244S) was 79% of that of the wt ($P < 0.005$) (Fig. 2A and Table 1), and its activation by sphingomyelin was only 3.6-fold (Fig. 2C and Table 1). The sphingomyelin binding of JFH1 (2a) RdRp(A242C) and RdRp(S244D) increased to 75.5% and 93.1%, respectively, of HCR6 (1b) RdRp wt (Fig. 2A and Table 1). This was significantly higher than that of JFH1 (2a) RdRp wt ($P < 0.005$), and the sphingomyelin activation of JFH1 (2a) RdRp(A242C) and RdRp(S244D) was increased 1.0-fold and 3.1-fold, respectively ($P < 0.005$) (Fig. 2C and Table 1). From these mutation analyses of the J6CF and JFH1 RdRps, we concluded that 244D enhanced sphingomyelin binding and RdRp activation.

HCV 1a RdRps were not activated even though sphingomyelin bound to them (Fig. 1E and 2A and Table 1). We then tried to elucidate the domains responsible for sphingomyelin activation. There are 14 amino acids (residues 19, 25, 81, 111, 120, 131, 184, 270, 272, 329, 436, 464, 487, and 540) unique to genotype 1a RdRp in the region of residues 1 to 570 and two amino acid differences unique to 1a RdRp in SBD, i.e., 238A and 248Q (see Fig. 6A). Initially, we focused on the SBD and introduced the A238S and Q248E mutations into the H77 (2a) RdRp SBD (Fig. 2A and D and Table 1). The sphingomyelin binding activity of H77 (2a) RdRp(A238S/Q248E) was similar to that of H77 (2a) RdRp wt. The sphingomyelin activation ratio of H77 (2a) RdRp(A238S/Q248E) was increased 8.1-fold, leading us to conclude that these mutations are essential to sphingomyelin activation.

Effect of lipids on HCV RNA polymerase activity. In order to elucidate the structure of the lipids involved in activation of HCV RdRp, D-lactosyl-β-1,1′-*N*-octanoyl-D-*erythro*-sphingosine [C_8-lactosyl(β) ceramide], D-glucosyl-β1-17-N-octanoyl-D-*erythro*-sphingosine (C_8-β-D-glucosyl ceramide), *N*-hexanol-D-*erythro*-sphingosine (C_6-ceramide), and cholesterol were tested for their abilities to activate RdRp. The relative polymerase activities of 100 nM HCV HCR6 (1b) RdRp activated with 0.01 mg/ml egg yolk sphingomyelin, 2 μM hexanoyl sphingomyelin, 8 μM C_8-lactosyl(β) ceramide, 12 μM C_8-β-D-glucosyl ceramide, 12 μM C_6-ceramide, and 0.02 mg/ml cholesterol were 11.2, 13.0, 5.66, 4.19, 1.12, and 2.25 of that without lipids, respectively (Fig. 3A). The amount of lipids that gave the maximum activation was calculated from the kinetics of the lipids bound to HCR6 (1b) and JFH1 (2a) RdRps (Fig. 3B and

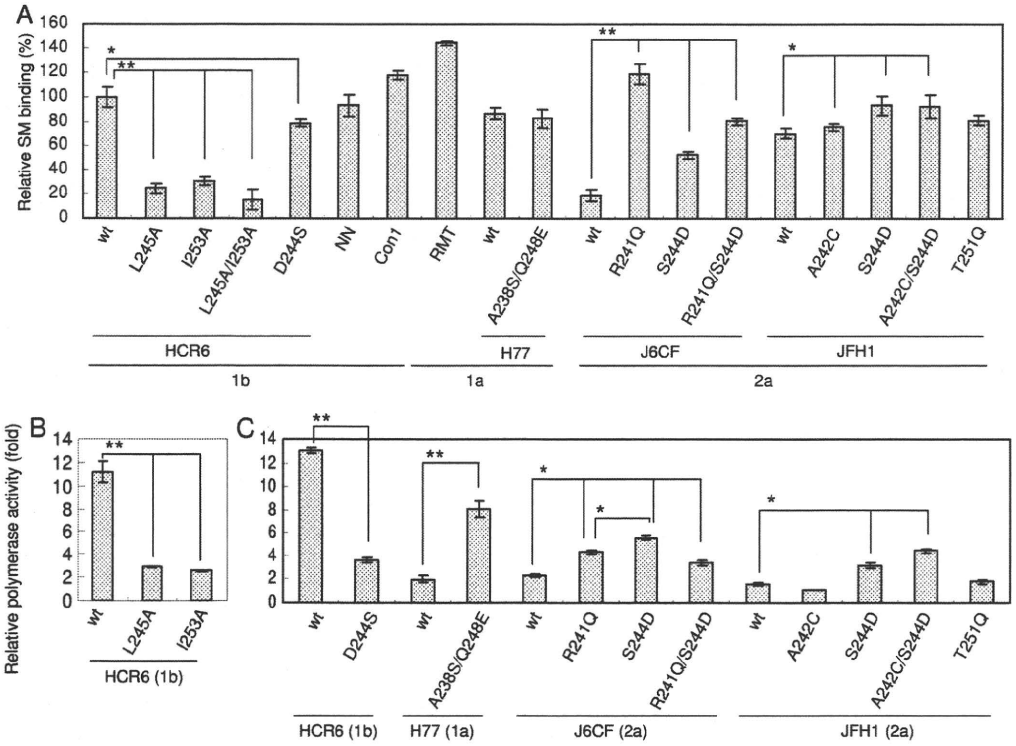

FIG. 2. Sphingomyelin binding and activation of HCV RNA polymerase sphingomyelin binding domain mutants. Names of RdRps are indicated below the graphs. (A) Egg yolk sphingomyelin (SM) binding activity relative to that of HCR6 (1b) RdRp wt. Mean ± standard deviation of the binding was calculated from three independent experiments. (B) Egg yolk sphingomyelin activation of HCR6 (1b) RdRps. RdRps (100 nM) were incubated with or without 0.01 mg/ml egg yolk sphingomyelin. (C) Hexanoyl sphingomyelin activation of the RdRps (RdRp names are indicated below the graphs). HCV RdRps (100 nM) were incubated with or without 2 μM hexanoyl sphingomyelin. The mean ± standard deviation of the activation ratio was calculated from three independent experiments. *, $P < 0.005$; ** $P < 0.001$.

C). C_8-lactosyl(β) ceramide and C_8-β-D-glucosyl ceramide activated HCR6 (1b) RdRp compared with the linear regression kinetics of the reaction with hexanoyl sphingomyelin as it plateaued (Fig. 1C and 3B). Cholesterol activated HCR6 (1b) RdRp slightly but did not activate JFH1 (2a) RdRp (Fig. 3C). We therefore concluded that the phosphocholine of sphingomyelin bound to the SBD of HCV RdRp because the order of HCV RdRp activation was hexanoyl sphingomyelin > C_8-lactosyl(β) ceramide > C_8-β-D-glucosyl ceramide, and C_6-ceramide did not activate HCV HCR6 (1b) RdRp. The polarity of the phosphocholine of sphingomyelin is important for HCV RdRp activation (see Fig. S5 in the supplemental material).

In order to test whether phosphocholine activated HCV RdRp (Fig. 3D), HCR6 (1b) RdRp was incubated with 0.4, 2, 20, 100, and 400 μg and 2, 4, 11, 54, and 100 mg of phosphocholine. Up to 400 μg of phosphocholine did not affect RdRp activity, but more than 2 mg of phosphocholine inhibited RdRp activity.

Effect of sphingomyelin on the template RNA binding of HCV RNA polymerase. The mechanism of HCV RdRp activation was analyzed. RNA polymerase changes its conformation throughout the different transcription steps, and template binding is the first step of transcription (9). Therefore, the effect of sphingomyelin on template RNA binding activity was tested (Fig. 4A and Table 1). Sphingomyelin enhanced the template RNA binding of HCR6 (1b) RdRp wt but not that of JFH1 (2a), H6CF (2a), or H77 (1a) wt RdRp. When the A238S/Q248E mutation was introduced into H77 (1a) RdRp, the RNA binding was enhanced. J6CF (2a) RdRp R241Q and S244D mutants showed similar enhancement of RNA binding, but the R241Q/S244D double mutant did not. The activation effect of RNA binding of HCR6 (1b) RdRp mutants L245A, I253A, and D244S was lower than that of RdRp wt. JFH1 (2a) RdRp wt and RdRp(A242C/S244D) showed similar RNA binding activation levels. Based on a comparison of the sphingomyelin activation of HCR6 (1b) RdRp wt and its mutants which lost sphingomyelin binding with J6CF (2a) RdRp wt and the R241Q and S244D mutants and H77 (1a) RdRp wt and the A238S/Q248E mutant, we concluded that polymerase activation by sphingomyelin was induced mainly via activation of the template RNA binding of RdRp. RNA binding activity of JFH1 (2a) RdRp wt and RdRp(A242C/S244D) was almost saturated because RNA binding of these RdRps was not activated by sphingomyelin (see Fig. S4 in the supplemental material).

HCV RdRp has to be bound with sphingomyelin before or at the same time as it binds to template RNA. After RdRp had bound to the template RNA, sphingomyelin did not enhance template RNA binding strongly (Fig. 4B).

Effect of the sphingomyelin binding domain mutations for HCV replicon activity with myriocin. In order to confirm sphingomyelin activation of HCV polymerase activity in a viral replication system, HCV replicon activity of the loss-of-function mutant HCV NN (1b) NS5B(D244S) and the gain-of-

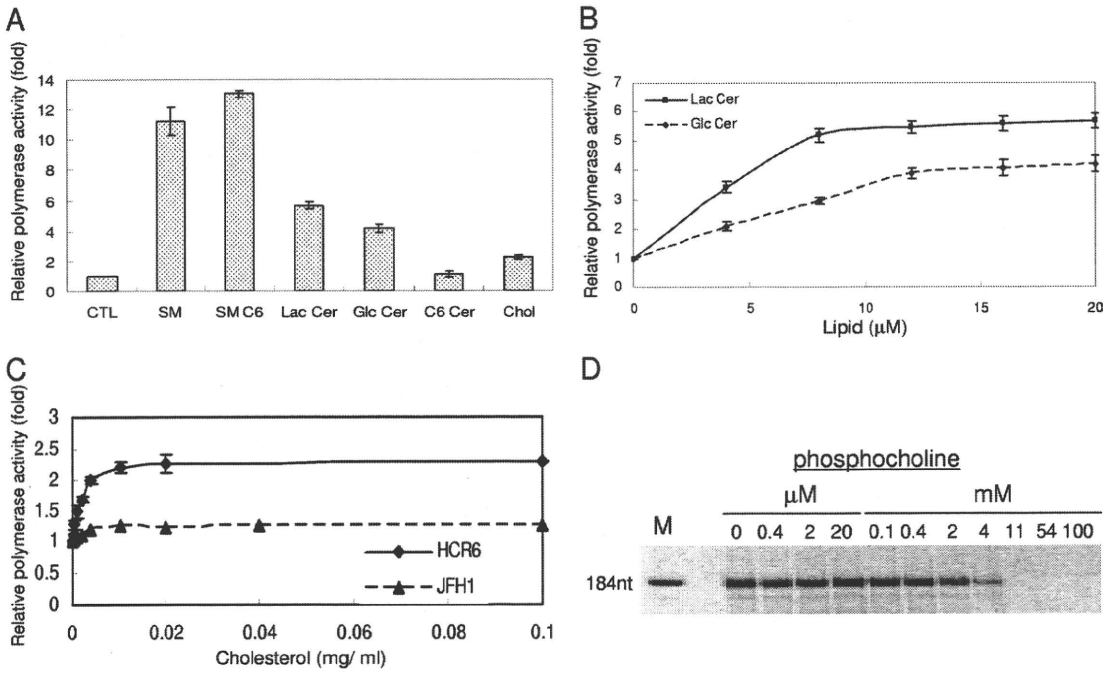

FIG. 3. HCV RNA polymerase activation effect of lipids. (A) Lipid activation of HCR6 (1b) RdRp wt. HCV HCR6 (1b) RdRp wt (100 nM) was incubated with or without (control [CTL]) 0.01 mg/ml egg yolk sphingomyelin (SM), 2 μM hexanoyl sphingomyelin (SM C6), 8 μM C_8-lactosyl(β) ceramide (Lac Cer), 12 μM C_8-β-D-glucosyl ceramide (Glc Cer), 12 μM C_6-ceramide (C6 Cer), or 0.02 mg/ml cholesterol (chol). (B) Activation kinetics of C_8-lactosyl(β) ceramide (Lac Cer) and C_8-β-D-glucosyl ceramide (Glc Cer) on HCR6 (1) RdRp. (C) Activation kinetics of cholesterol on HCR6 (1b) and JFH1 (12a) RdRps. (D) The effect of phosphocholine on HCR6 (1b) RdRp. The mean ± standard deviation of the activation ratio was calculated from three independent experiments.

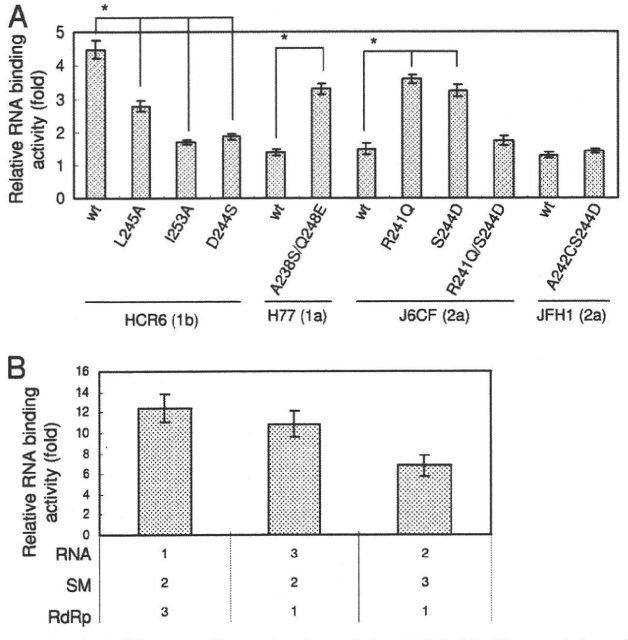

FIG. 4. Sphingomyelin activation of the RNA binding activity of HCV RNA polymerase. (A) Sphingomyelin activation of RNA filter binding of HCV RdRps (RdRp names are indicated below the graph). RdRps and ^{32}P-labeled RNA template (SL12-1S) were incubated with or without egg yolk sphingomyelin (SM), before filtration. (B) Effect of the order of sphingomyelin treatment. Numbers below the graph indicate the order in which the reagents were added. The graph represents the ratio to RNA binding without sphingomyelin. The mean ± standard deviation of the activation ratio was calculated from three independent experiments. *, $P < 0.01$.

function mutants H77 (1a) NS5B(A238S/Q248E) and JFH1 (2a) NS5B(A242C/S244D) were compared with 5 and 50 nM myriocin treatment for 72 h (Fig. 5).

First, HCV replicon activity was compared as the relative luciferase activity (Fig. 5A). Both JFH1 (2a) wt and NS5B(A242C/S244D) replicons showed similar and strong replicon activity ($133 \times 10^3 \pm 12 \times 10^3$ and $138 \times 10^3 \pm 8.5 \times 10^3$, respectively). JFH1 (2a) wt replicon was resistant to myriocin treatment, as reported by Aizaki et al. using other SPT inhibitors (3). The JFH1 (2a) NS5B(A242C/S244D) replicon became sensitive to myriocin but still showed higher replicon activity than NN (1b) or H77 (1a) replicons even at 50 nM myriocin.

To analyze the effect of mutations precisely, the replicon activity relative to each wt strain was compared (Fig. 5B). The JFH1 (2a) wt replicon with 50 nM myriocin showed the same luciferase activity as the wt without myriocin (102% ± 9.6%). JFH1 (2a) NS5B(A242C/S244D) replicon activity was the same as that of the wt without myriocin (103% ± 12%); with 5 nM myriocin it was 84.1% ± 6.6% of the wt level, but with 50 nM myriocin it was 70.3% ± 5.3% of the wt level, which was significantly lower ($P < 0.01$). NN (1b) wt replicon activity was 45.3% ± 6.6% with 5 nM myriocin and 21.7% ± 2.9% with 50 nM myriocin relative to the wt level without myriocin. NN (1b) NS5B(D244S) replicon activity was 72.2% ± 12% without myriocin ($P < 0.05$), 44.0% ± 7.4% with 5 nM myriocin, and 38.1% ± 4.2% with 50 nM myriocin relative to wt level without myriocin, which was significantly higher ($P < 0.01$). Thus, NN (1b) NS5B(D244S) showed lower replicon activity than the wt

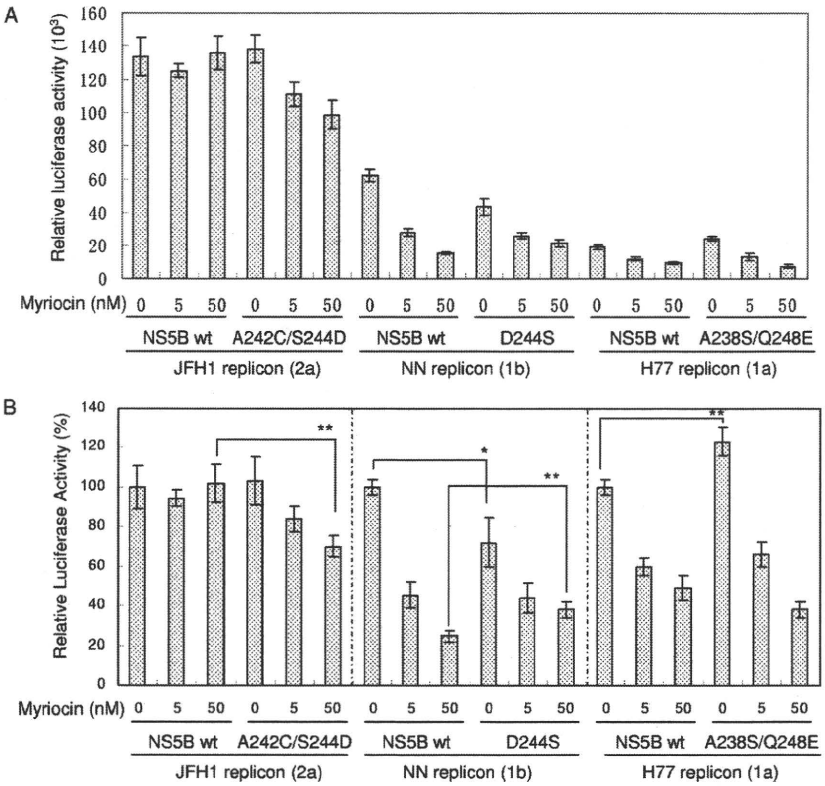

FIG. 5. Myriocin inhibition of HCV replicon activity. Huh7.5.1 cells were incubated with myriocin after transfection with the HCV replicons indicated below the graphs. Means ± standard deviations of the relative luciferase activity at 72 h after myriocin treatment compared to activity at 4 h after transfection (A) and to that of each wt without myriocin (B) were calculated from three independent measurements. *, $P < 0.05$; ** $P < 0.01$.

and was less sensitive to myriocin than the wt. H77 (1a) wt replicon activity was 59.9% ± 4.2% with 5 nM myriocin and 49.2% ± 6.4% with 50 nM myriocin relative to the wt level without myriocin. H77 (1a) NS5B(A238S/Q248E) replicon activity was 123% ± 7.1% without myriocin ($P < 0.01$), 66.1% ± 6.3% with 5 nM myriocin, and 38.0% ± 4.1% with 50 nM myriocin relative to wt level without myriocin. Both H77 (1a) wt and NS5B(A238S/Q248E) replicons were sensitive to myriocin, and the replicon activity of NS5B(A238S/Q248E) was higher than that of the wt.

JFH1 (2a) RdRp(A242C/S244D) localized in the DRM fractions. Myriocin sensitivity of JFH1 (2a) NS5B(A242C/S244D) replicon indicates the importance of 244D in JFH1 NS5B for sphingomyelin binding. To further confirm the role of 244D for recruitment of HCV RdRp to the detergent-resistant membrane (DRM), where the HCV replication complex exists, we compared the distribution of NS5A and NS5B of JFH1 (2a) wt and NS5B(A242C/S244D) in their replicon cells by sucrose density gradient centrifugation of the DRM (Fig. 6). NS5A proteins of both JFH1 (2a) wt and NS5B(A242C/S244D) replicons localized in the DRM fraction where caveolin-2 was present (11, 27), but most of NS5B wt localized in the Triton-soluble fractions. NS5B of JFH1 (2a) NS5B(A242C/S244D) replicon was shifted to the DRM fraction from the soluble fraction. The shift of NS5B(A242C/S244D) localization into the DRM demonstrated that SBD was the DRM localization domain of NS5B and that residue 244D was important for this localization.

DISCUSSION

Hepatitis C virus is an envelope virus, and the lipid components of the virion play important roles in HCV infectivity and virion assembly (3, 15, 20, 24). HCV replication complexes localize in lipid raft structures/DRMs in the membrane frac-

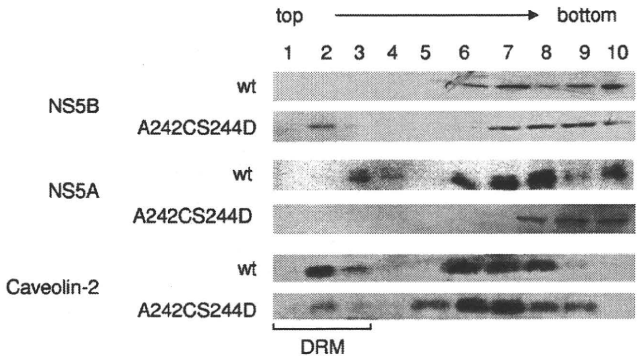

FIG. 6. Membrane floating assay of JFH1 wt and NS5B(A242C/S244D) replicon cells. The PNS fractions of HCV JFH1 (2a) wt and NS5B(A242C/S244D) replicon cells were treated with 1% Triton X-100 in TNE buffer for 30 min at 4°C and subjected to 10 to 40% sucrose gradient centrifugation in TNE buffer. Each fraction was subjected to 10% SDS-PAGE, followed by Western blotting with anti-NS5A, -NS5B, and -caveolin-2 antibodies. Fractions are numbered as indicated at the top of the panel. The DRM fractions (fractions 1 to 3) are indicated.

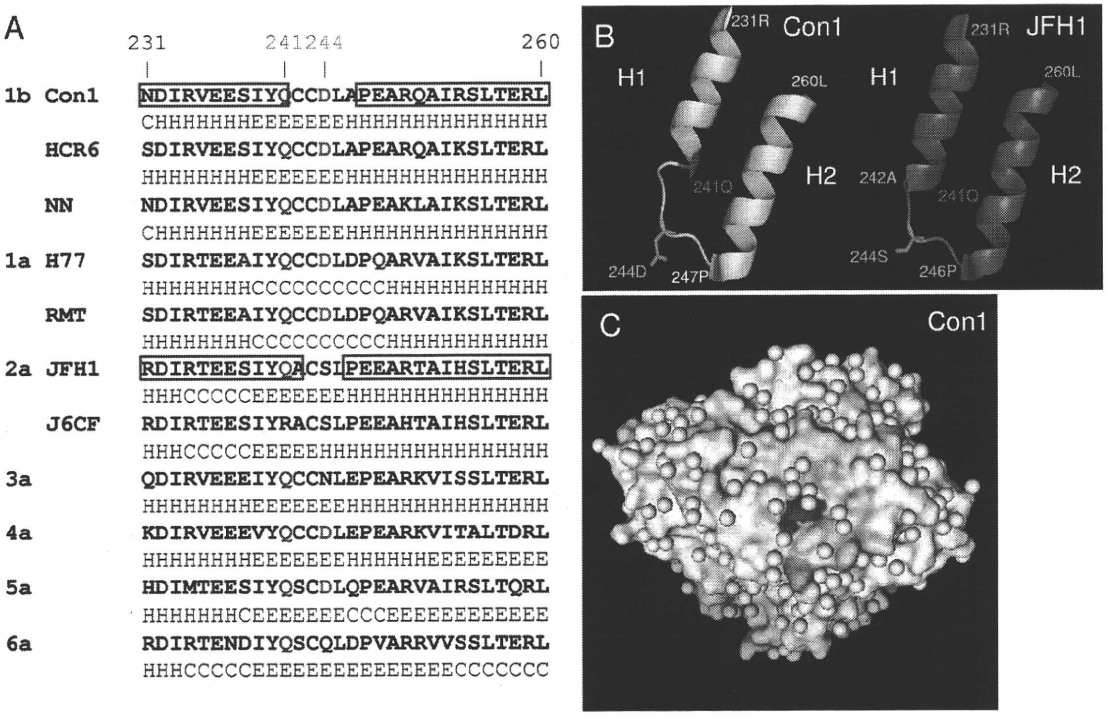

FIG. 7. Sphingomyelin binding domain (SBD) of HCV RNA polymerase. (A) The SBDs (231N to 260L) of HCV RdRps are aligned together with their secondary structure predicted by the Chou-Fasman program (10). The predicted secondary structure is indicated below the sequence as follows: H, α-helix; E, β-sheet; and C, coil. The α-helix structures of HCV Con1 (1b) RdRp and JFH1 (2a) RdRp are boxed in red. Residues 241Q and 244D are indicated in red and green, respectively. The 238A and 248E of the H77 and RMT (1a) RdRps are indicated in purple. GenBank accession numbers of HCV genotypes 3a, 4a, 5a, and 6a are GU814263 (12), GU814265 (12), Y13184 (8), and Y12083 (1), respectively. (B) Comparison of the SBDs of HCV Con1 (1b) (yellow) and JFH1 (2a) RdRps (magenta). The starting and ending amino acids of H1 and H2 are indicated. The sphingomyelin binding site, 241Q, is indicated in red, and 244D of Con1 (1b) and 244S of JFH1 (2a) RdRp are indicated in green. (C) Surface model of HCV Con1 (1b) RdRp. SBD is indicated in yellow, and 241Q and 244D are indicated in red and green, respectively. The structures of the Con1 and JFH1 RdRps were constructed by PyMOL, version 1.1.1 (http://www.pymol.org/). PDB numbers of Con1 (1b) RdRp and JFH1 (2a) RdRp are 3FQL (14) and 3I5K (31), respectively.

tions of subgenomic replicon cells (30). Lipid rafts are composed mainly of sphingomyelin, cholesterol, and glycosphingolipids. Most reports regarding the relationship between lipids and HCV have examined virion assembly, infectivity, and the localization of HCV, but their biochemical interactions have not been reported. Our findings clearly demonstrate that sphingomyelin plays an important role not only in HCV replication complex formation and its localization but also in HCV RdRp activity.

The helix-turn-helix structure of the SBD (residues 230 to 263), which is located between RNA polymerase motifs A and B, has been proposed as the sphingomyelin binding domain of HCV RdRp (29). We compared the SBD of Con1 (1b) (Protein Data Bank [PDB] 3FQL) (14) and JFH1 (2a) (PDB 3I5K) (31) and the secondary structure of the amino acids (201 to 290) in the SBD predicted by the Chou-Fasman program (10) (Fig. 7; see also Fig. S5 in the supplemental material) because the helix structures of the SBD of Con1 (helix 1 [H1], 231N to 241Q; helix 2 [H2], 247A to 260L) and JFH1 (H1, 231R to 242A; H2, 246P to 260L) RdRp fit with those predicted by the Chou-Fasman program. The structures contributing to sphingomyelin binding and activation are H1 and H2 and the junction (turn) between the two helix structures that are similar to the human immunodeficiency virus (HIV) gp120 V3 domain, prion protein (PrP), and β-amyloid peptide (13, 22). Although Con1 (1b) RdRp has a shorter helix structure than JFH1 (2a) RdRp (Fig. 6B), the structures of their SBDs are very similar (Fig. 7; see also Fig. S5). When the helix-turn-helix structure of the SBD was destroyed (HCR6 genotype 1b RdRp mutants L245A and I253A), the RdRp lost sphingomyelin binding activity and lost its activation (Fig. 2).

In order to study the structure-function relationship of the SBD and sphingomyelin, we compared the SBD of genotype 1a, 1b and 2a RdRps and particularly focused on residue 244D in the turn and residues 241Q and 238S/248E in the helix domains. The polar amino acid 241Q and the negatively charged 244D of Con1 (1b) RdRp located on the surface of the RdRp molecule bind and interact with the positively charged choline residue of sphingomyelin (Fig. 7C; see also Fig. S5 in the supplemental material). The positively charged 241R repels the choline residue of sphingomyelin, and as a result, J6CF (a) RdRp wt did not bind to sphingomyelin. J6CF (2a) RdRp(R241Q) showed almost the same sphingomyelin binding activity as HCR6 (1b) RdRp wt. This ionic interaction between SBD and sphingomyelin agrees with the activation of lipids with different sphingosine structures and fatty acid chains (Fig. 3A). JFH1 (2a) RdRp does not interact well with sphingomyelin because it does not have the negatively charged

amino acids at the tip of its turn structure. Once its 244S was changed to D, more sphingomyelin bound to JFH1 (2a) RdRp and activated the RdRp (Fig. 2A and C). The reason for the low activation of J6CF (2a) RdRp(R241Q/S244D) is not clear. Sometimes mutations affect the entire conformation of the molecule. In conclusion, from the comparison of sphingomyelin binding and activation of HCR6 (1b), J6CF (2a), and JFH1 (2a) RdRp SBD mutants, 241Q is the essential amino acid for sphingomyelin binding in the SBD. Amino acid 244D enhanced both binding and RdRp activation.

The *in vitro* sphingomyelin binding and RdRp activation experiments indicate that sphingomyelin binding and its RdRp activation are different biochemical reactions because we found controversial activation rates for sphingomyelin binding and RdRp activation among J6CF (2a) RdRp mutants (Fig. 2). The relationship between sphingomyelin binding and the activation of polymerase activity was studied by comparing genotype 1b and 1a RdRps, both of which bind to sphingomyelin (Fig. 2). However, 1a RdRp is not activated by sphingomyelin because both of the helix structures of 1a RdRp are probably terminated at 238A and 248Q, making its helix structures shorter than those of 1b RdRp (Fig. 6A). The length of the helix structure may be essential for sphingomyelin activation because RdRp changes its structure to bind to template RNA when sphingomyelin binds to SBD (Fig. 4).

HCV RdRp changes its conformations at the early stages of transcription initiation, including the template RNA binding step (6, 9). Sphingomyelin binding is likely to change the conformation of 1b RdRp to recruit template RNA and initiate transcription efficiently. Comparison of the activation ratio of RNA binding and polymerase activity of 1b RdRp, J6CF (2a) RdRp wt and R241Q and S244D mutants, and JFH1 (2a) RdRp wt and mutant A242C/S244D suggests that steps other than RNA binding are also likely to be activated by sphingomyelin.

From a kinetic analysis of sphingomyelin activation (Fig. 1C and D), 20 sphingomyelin molecules are estimated to interact with the SBD of RdRp and activate it because sphingomyelin activation plateaued at 20 sphingomyelin molecules per HCV RdRp molecule. It is not clear whether 20 sphingomyelin molecules form a micelle or a layer structure. However, the structure of sphingomyelin is important for the activation of HCV RdRp because phosphocholine did not activate the RdRp (Fig. 3D).

To confirm these biochemical findings in HCV replication, we tested the effect of SBD mutations in HCV replicon systems with the SPT inhibitor myriocin (Fig. 5) (4, 33) because NA255 was not available. The loss-of-function mutant, HCV NN (1b) NS5B(D244S), showed lower replicon activity than NN (1b) wt and more resistance to 50 nM myriocin, which did not affect the viability of cells (4, 33), than the wt. The gain-of-function mutant, H77 (1a) NS5B(A238S/Q248E), showed higher replicon activity than H77 wt and retained myriocin sensitivity because it had the sphingomyelin binding sites 241Q and 244D. At 50 nM myriocin, another gain-of-function mutant, JFH1 (2a) NS5B(A242C/S244D), was inhibited although its activity was the same as that of JFH1 (2a) wt without myriocin because the JFH1 wt replicon had high replicon activity without myriocin (Fig. 5A). The JFH1 replicon activity may be maximal in the system; therefore, the JFH1 (2a) NS5B(A242C/S244D) replicon did not show higher activity than JFH1 (2a) wt without myriocin while H77 (1a) NS5B(A238S/Q248E) showed higher replicon activity than H77 wt.

The binding and RdRp activation activity of the amino acid 244 mutants by sphingomyelin did not differ greatly from the wt *in vitro*. However, the myriocin sensitivity of JFH1 (2a) NS5B(S244D) was demonstrated clearly. That of H77 (1a) NS5B(A238S/Q248E) indicated that sphingomyelin binding was the target of myriocin inhibition, not the sphingomyelin activation of RdRp. These data confirm the importance of 241Q, 244D, and the helix structure in SBD for HCV replication in the cells.

Sphingomyelin is the major component of the lipid raft structure/DRM where the HCV genome replicates. To confirm that the SBD is the membrane binding site of HCV RdRp, we analyzed the localization of NS5B of JFH1 (2a) wt and NS5B(A242C/S244D) replicons by membrane floating assay (Fig. 6). JFH1 (2a) NS5B wt did not localize in the DRM. However, the localization of NS5B of the JFH1 (2a) NS5B(A242C/S244D) replicon shifted to the DRM from the soluble fractions. Previously, HCV NS5B was believed to localize in the DRM by its C-terminal hydrophobic sequences (21). However, our data demonstrate that the SBD is the membrane localization domain of HCV NS5B, which agrees with the myriocin sensitivity of JFH1 (2a) NS5B(A242C/S244D) replicons (Fig. 5) and the release of HCV 1b NS5B from the DRM by another SPT inhibitor, NA255 (29).

This is the first report of RNA polymerase activation by lipids. Twenty sphingomyelin molecules interact with SBD, particularly with residues 241Q and 244D of HCV (1b) RdRp, and change the conformation of the RdRp in order to recruit RNA templates. At the same time, HCV RdRp molecules may be aligned on the sphingomyelin layer formed via interactions between the hydrocarbon chains of sphingosine and fatty acids via placement of their SBD into the layer (Fig. 7C). Consistent with previous research (3, 23, 37), our findings explain why the inhibitors of the sphingolipid biosynthetic pathway influence subgenomic replicons derived from HCV genotypes 1a and 1b but not those derived from JFH1 (2a) (Fig. 5). Most HCV isolates have 241Q in NS5B, and some of them also have 244D (Fig. 7A). These sphingomyelin interactions are new targets for the treatment of HCV.

ACKNOWLEDGMENTS

We thank C. Rice and R. Bartenshlager for the HCV H77 and Con1 plasmids, respectively. We also thank F. Chisari for Huh7.5.1 and Huh7/src cells.

This work was supported by a grant-in-aid from the Chinese Academy of Sciences (O514P51131 and KSCX1-YW-10), the Chinese 973 project (2009CB522504), and the Chinese National Science and Technology Major Project (2008ZX10002-014).

REFERENCES

1. **Adams, N. J., R. W. Chamberlain, L. A. Taylor, F. Davidson, C. K. Lin, R. M. Elliott, and P. Simmonds.** 1997. Complete coding sequence of hepatitis C virus genotype 6a. Biochem. Biophys. Res. Commun. **234:**393–396.
2. **Aizaki, H., K. J. Lee, V. M. Sung, H. Ishiko, and M. M. Lai.** 2004. Characterization of the hepatitis C virus RNA replication complex associated with lipid rafts. Virology **324:**450–461.
3. **Aizaki, H., K. Morikawa, M. Fukasawa, H. Hara, Y. Inoue, H. Tani, K. Saito, M. Nishijima, K. Hanada, Y. Matsuura, M. M. Lai, T. Miyamura, T. Wakita, and T. Suzuki.** 2008. Critical role of virion-associated cholesterol and sphingolipid in hepatitis C virus infection. J. Virol. **82:**5715–5724.
4. **Amemiya, F., S. Maekawa, Y. Itakura, A. Kanayama, A. Matsui, S. Takano, T. Yamaguchi, J. Itakura, T. Kitamura, T. Inoue, M. Sakamoto, K. Yamau-**

chi, S. Okada, A. Yamashita, N. Sakamoto, M. Itoh, and N. Enomoto. 2008. Targeting lipid metabolism in the treatment of hepatitis C virus infection. J. Infect. Dis. **197:**361–370.

5. **Binder, M., D. Quinkert, O. Bochkarova, R. Klein, N. Kezmic, R. Bartenschlager, and V. Lohmann.** 2007. Identification of determinants involved in initiation of hepatitis C virus RNA synthesis by using intergenotypic replicase chimeras. J. Virol. **81:**5270–5283.
6. **Biswal, B. K., M. M. Cherney, M. Wang, L. Chan, C. G. Yannopoulos, D. Bilimoria, O. Nicolas, J. Bedard, and M. N. James.** 2005. Crystal structures of the RNA-dependent RNA polymerase genotype 2a of hepatitis C virus reveal two conformations and suggest mechanisms of inhibition by non-nucleoside inhibitors. J. Biol. Chem. **280:**18202–18210.
7. **Blight, K. J., J. A. McKeating, J. Marcotrigiano, and C. M. Rice.** 2003. Efficient replication of hepatitis C virus genotype 1a RNAs in cell culture. J. Virol. **77:**3181–3190.
8. **Chamberlain, R. W., N. J. Adams, L. A. Taylor, P. Simmonds, and R. M. Elliott.** 1997. The complete coding sequence of hepatitis C virus genotype 5a, the predominant genotype in South Africa. Biochem. Biophys. Res. Commun. **236:**44–49.
9. **Chinnaswamy, S., I. Yarbrough, S. Palaninathan, C. T. Kumar, V. Vijayaraghavan, B. Demeler, S. M. Lemon, J. C. Sacchettini, and C. C. Kao.** 2008. A locking mechanism regulates RNA synthesis and host protein interaction by the hepatitis C virus polymerase. J. Biol. Chem. **283:**20535–20546.
10. **Chou, P. Y., and G. D. Fasman.** 1974. Prediction of protein conformation. Biochemistry **13:**222–245.
11. **Fujimoto, T., H. Kogo, K. Ishiguro, K. Tauchi, and R. Nomura.** 2001. Caveolin-2 is targeted to lipid droplets, a new "membrane domain" in the cell. J. Cell Biol. **152:**1079–1085.
12. **Gottwein, J. M., T. K. Scheel, B. Callendret, Y. P. Li, H. B. Eccleston, R. E. Engle, S. Govindarajan, W. Satterfield, R. H. Purcell, C. M. Walker, and J. Bukh.** Novel infectious cDNA clones of hepatitis C virus genotype 3a (strain S52) and 4a (strain ED43): genetic analyses and *in vivo* pathogenesis studies. J. Virol. **84:**5277–5293.
13. **Hammache, D., G. Pieroni, N. Yahi, O. Delezay, N. Koch, H. Lafont, C. Tamalet, and J. Fantini.** 1998. Specific interaction of HIV-1 and HIV-2 surface envelope glycoproteins with monolayers of galactosylceramide and ganglioside GM3. J. Biol. Chem. **273:**7967–7971.
14. **Hang, J. Q., Y. Yang, S. F. Harris, V. Leveque, H. J. Whittington, S. Rajyaguru, G. Ao-Ieong, M. F. McCown, A. Wong, A. M. Giannetti, S. Le Pogam, F. Talamas, N. Cammack, I. Najera, and K. Klumpp.** 2009. Slow binding inhibition and mechanism of resistance of non-nucleoside polymerase inhibitors of hepatitis C virus. J. Biol. Chem. **284:**15517–15529.
15. **Huang, H., F. Sun, D. M. Owen, W. Li, Y. Chen, M. Gale, Jr., and J. Ye.** 2007. Hepatitis C virus production by human hepatocytes dependent on assembly and secretion of very low-density lipoproteins. Proc. Natl. Acad. Sci. U. S. A. **104:**5848–5853.
16. **Ishii, N., K. Watashi, T. Hishiki, K. Goto, D. Inoue, M. Hijikata, T. Wakita, N. Kato, and K. Shimotohno.** 2006. Diverse effects of cyclosporine on hepatitis C virus strain replication. J. Virol. **80:**4510–4520.
17. **Kashiwagi, T., K. Hara, M. Kohara, K. Kohara, J. Iwahashi, N. Hamada, H. Yoshino, and T. Toyoda.** 2002. Kinetic analysis of C-terminally truncated RNA-dependent RNA polymerase of hepatitis C virus. Biochem. Biophys. Res. Commun. **290:**1188–1194.
18. **Kato, T., T. Date, M. Miyamoto, A. Furusaka, K. Tokushige, M. Mizokami, and T. Wakita.** 2003. Efficient replication of the genotype 2a hepatitis C virus subgenomic replicon. Gastroenterology **125:**1808–1817.
19. **Kiyosawa, K., T. Sodeyama, E. Tanaka, Y. Gibo, K. Yoshizawa, Y. Nakano, S. Furuta, Y. Akahane, K. Nishioka, R. H. Purcell, et al.** 1990. Interrelationship of blood transfusion, non-A, non-B hepatitis and hepatocellular carcinoma: analysis by detection of antibody to hepatitis C virus. Hepatology **12:**671–675.
20. **Lambot, M., S. Fretier, A. Op De Beeck, B. Quatannens, S. Lestavel, V. Clavey, and J. Dubuisson.** 2002. Reconstitution of hepatitis C virus envelope glycoproteins into liposomes as a surrogate model to study virus attachment. J. Biol. Chem. **277:**20625–20630.
21. **Lemon, S., C. Walker, M. Alter, and M. Yi.** 2007. Hepatitis C virus, p. 1253–1304. *In* D. M. Knipe, P. M. Howley, D. E. Griffin, R. A. Lamb, M. A. Martin, B. Roizman, and S. E. Straus (ed.), Fields virology, 5th ed. Lippincott Williams & Wilkins, Philadelphia, PA.
22. **Mahfoud, R., N. Garmy, M. Maresca, N. Yahi, A. Puigserver, and J. Fantini.** 2002. Identification of a common sphingolipid-binding domain in Alzheimer, prion, and HIV-1 proteins. J. Biol. Chem. **277:**11292–11296.
23. **Miyake, Y., Y. Kozutsumi, S. Nakamura, T. Fujita, and T. Kawasaki.** 1995. Serine palmitoyltransferase is the primary target of a sphingosine-like immunosuppressant, ISP-1/myriocin. Biochem. Biophys. Res. Commun. **211:** 396–403.
24. **Miyanari, Y., K. Atsuzawa, N. Usuda, K. Watashi, T. Hishiki, M. Zayas, R. Bartenschlager, T. Wakita, M. Hijikata, and K. Shimotohno.** 2007. The lipid droplet is an important organelle for hepatitis C virus production. Nat. Cell Biol. **9:**1089–1097.
25. **Murayama, A., T. Date, K. Morikawa, D. Akazawa, M. Miyamoto, M. Kaga, K. Ishii, T. Suzuki, T. Kato, M. Mizokami, and T. Wakita.** 2007. The NS3 helicase and NS5B-to-3′X regions are important for efficient hepatitis C virus strain JFH-1 replication in Huh7 cells. J. Virol. **81:**8030–8040.
26. **Murayama, A., L. Weng, T. Date, D. Akazawa, X. Tian, T. Suzuki, T. Kato, Y. Tanaka, M. Mizokami, T. Wakita, and T. Toyoda.** 2010. RNA polymerase activity and specific RNA structure are required for efficient HCV replication in cultured cells. PLoS Pathog. **6:**e1000885.
27. **Ostermeyer, A. G., J. M. Paci, Y. Zeng, D. M. Lublin, S. Munro, and D. A. Brown.** 2001. Accumulation of caveolin in the endoplasmic reticulum redirects the protein to lipid storage droplets. J. Cell Biol. **152:**1071–1078.
28. **Saito, I., T. Miyamura, A. Ohbayashi, H. Harada, T. Katayama, S. Kikuchi, Y. Watanabe, S. Koi, M. Onji, Y. Ohta, et al.** 1990. Hepatitis C virus infection is associated with the development of hepatocellular carcinoma. Proc. Natl. Acad. Sci. U. S. A. **87:**6547–6549.
29. **Sakamoto, H., K. Okamoto, M. Aoki, H. Kato, A. Katsume, A. Ohta, T. Tsukuda, N. Shimma, Y. Aoki, M. Arisawa, M. Kohara, and M. Sudoh.** 2005. Host sphingolipid biosynthesis as a target for hepatitis C virus therapy. Nat. Chem. Biol. **1:**333–337.
30. **Shi, S. T., K. J. Lee, H. Aizaki, S. B. Hwang, and M. M. Lai.** 2003. Hepatitis C virus RNA replication occurs on a detergent-resistant membrane that cofractionates with caveolin-2. J. Virol. **77:**4160–4168.
31. **Simister, P., M. Schmitt, M. Geitmann, O. Wicht, U. H. Danielson, R. Klein, S. Bressanelli, and V. Lohmann.** 2009. Structural and functional analysis of hepatitis C virus strain JFH1 polymerase. J. Virol. **83:**11926–11939.
32. **Tsukiyama-Kohara, K., S. Tone, I. Maruyama, K. Inoue, A. Katsume, H. Nuriya, H. Ohmori, J. Ohkawa, K. Taira, Y. Hoshikawa, F. Shibasaki, M. Reth, Y. Minatogawa, and M. Kohara.** 2004. Activation of the CKI-CDK-Rb-E2F pathway in full genome hepatitis C virus-expressing cells. J. Biol. Chem. **279:**14531–14541.
33. **Umehara, T., M. Sudoh, F. Yasui, C. Matsuda, Y. Hayashi, K. Chayama, and M. Kohara.** 2006. Serine palmitoyltransferase inhibitor suppresses HCV replication in a mouse model. Biochem. Biophys. Res. Commun. **346:**67–73.
34. **Wasley, A., and M. J. Alter.** 2000. Epidemiology of hepatitis C: geographic differences and temporal trends. Semin. Liver Dis. **20:**1–16.
35. **Watashi, K., N. Ishii, M. Hijikata, D. Inoue, T. Murata, Y. Miyanari, and K. Shimotohno.** 2005. Cyclophilin B is a functional regulator of hepatitis C virus RNA polymerase. Mol. Cell **19:**111–122.
36. **Weng, L., J. Du, J. Zhou, J. Ding, T. Wakita, M. Kohara, and T. Toyoda.** 2009. Modification of hepatitis C virus 1b RNA polymerase to make a highly active JFH1-type polymerase by mutation of the thumb domain. Arch. Virol. **154:**765–773.
37. **Yasuda, S., H. Kitagawa, M. Ueno, H. Ishitani, M. Fukasawa, M. Nishijima, S. Kobayashi, and K. Hanada.** 2001. A novel inhibitor of ceramide trafficking from the endoplasmic reticulum to the site of sphingomyelin synthesis. J. Biol. Chem. **276:**43994–44002.
38. **Zhong, J., P. Gastaminza, G. Cheng, S. Kapadia, T. Kato, D. R. Burton, S. F. Wieland, S. L. Uprichard, T. Wakita, and F. V. Chisari.** 2005. Robust hepatitis C virus infection in vitro. Proc. Natl. Acad. Sci. U. S. A. **102:**9294–9299.

JOURNAL OF VIROLOGY, Mar. 2010, p. 2798–2807 Vol. 84, No. 6
0022-538X/10/$12.00 doi:10.1128/JVI.02499-09

Involvement of Ceramide in the Propagation of Japanese Encephalitis Virus▽

Hideki Tani, Mai Shiokawa, Yuuki Kaname, Hiroto Kambara, Yoshio Mori, Takayuki Abe, Kohji Moriishi, and Yoshiharu Matsuura*

Department of Molecular Virology, Research Institute for Microbial Diseases, Osaka University, Osaka, Japan

Received 27 November 2009/Accepted 22 December 2009

Japanese encephalitis virus (JEV) is a mosquito-borne RNA virus and one of the most important flaviviruses in the medical and veterinary fields. Although cholesterol has been shown to participate in both the entry and replication steps of JEV, the mechanisms of infection, including the cellular receptors of JEV, remain largely unknown. To clarify the infection mechanisms of JEV, we generated pseudotype (JEVpv) and recombinant (JEVrv) vesicular stomatitis viruses bearing the JEV envelope protein. Both JEVpv and JEVrv exhibited high infectivity for the target cells, and JEVrv was able to propagate and form foci as did authentic JEV. Anti-JEV envelope antibodies neutralized infection of the viruses. Treatment of cells with inhibitors for vacuolar ATPase and clathrin-mediated endocytosis reduced the infectivity of JEVpv, suggesting that JEVpv enters cells via pH- and clathrin-dependent endocytic pathways. Although treatment of the particles of JEVpv, JEVrv, and JEV with cholesterol drastically reduced the infectivity as previously reported, depletion of cholesterol from the particles by treatment with methyl β-cyclodextrin enhanced infectivity. Furthermore, treatment of cells with sphingomyelinase (SMase), which hydrolyzes membrane-bound sphingomyelin to ceramide, drastically enhanced infection with JEVpv and propagation of JEVrv, and these enhancements were inhibited by treatment with an SMase inhibitor or C_6-ceramide. These results suggest that ceramide plays crucial roles in not only entry but also egress processes of JEV, and they should assist in the clarification of JEV propagation and the development of novel therapeutics against diseases caused by infection with flaviviruses.

Japanese encephalitis virus (JEV) is a small, enveloped virus belonging to the family *Flaviviridae* and the genus *Flavivirus*, which also includes *Dengue virus* (DENV), *West Nile virus* (WNV), *Yellow fever virus*, and *Tick-borne encephalitis virus* (11). JEV is the most common agent of viral encephalitis, causing approximately 50,000 cases annually, of which 15,000 will die, and up to 50% of survivors are left with severe residual neurological complications. JEV has a single-stranded positive-sense RNA genome of approximately 11 kb, encoding a single large polyprotein, which is cleaved by the host- and virus-encoded proteases into three structural proteins, capsid (C), premembrane (PrM), and envelope (E), and seven nonstructural proteins. The structural proteins are components of viral particles, and the E protein is suggested to interact with a cell surface receptor molecule(s). Although a number of cellular components, including heat shock cognate protein 70 (33), glycosaminoglycans, such as heparin or heparan sulfate (21, 41), and laminin (3), have been shown to participate in JEV infection, the precise mechanisms by which these receptor candidates participate in JEV infection remain largely unclear.

In addition to the many studies identifying and characterizing receptor molecules in numerous viruses, data suggesting the involvement of membrane lipids, such as sphingolipids and cholesterol, in viral infection have also been accumulating. Lipid rafts consisting of sphingolipids and cholesterol and distributing to the outer leaflet of the cell membrane have been shown to be involved in the infection of not only many viruses but also several bacteria and parasites (24), in addition to playing roles in various functions such as lipid sorting, protein trafficking (26, 47), cell polarity, and signal transduction (38). With respect to cholesterol itself, various aspects of the life cycle of flaviviruses have been shown to involve this lipid, including the entry of DENV (34), hepatitis C virus (HCV) (16), and WNV (27), the membrane fusion of tick-borne encephalitis virus (40), and the replication of HCV (14, 17), WNV (23), and DENV (35). Recently Lee et al. (20) showed that treatment with cholesterol efficiently impairs both the entry and replication steps of JEV and DENV-2 but enhances infection with the Sindbis virus (22).

On the other hand, sphingolipids, including sphingomyelins and glycosphingolipids, are ubiquitous components of eukaryotic cell membrane structures, providing integrity to cellular membranes. Ceramide is one of the intermediates of sphingolipids and plays roles in cell differentiation, regulation of apoptosis and protein secretion, induction of cellular senescence, and other processes (2). Ceramide is generated from the hydrolysis of sphingomyelin by sphingomyelinase (SMase) or from catalysis by serine-palmitoyl-coenzyme A (CoA) transferase and ceramide synthase. Ceramide spontaneously self-associates to form ceramide-enriched microdomains and then to form larger ceramide-enriched membrane platforms which serve as the spatial and temporal organization for cellular signalosomes and for regulation of protein functions (2). The ceramide-enriched platforms have also been used by many pathogens to facilitate entry and infection (2). The acid SMase is activated not only by multiple stimuli, including receptor molecules, gamma irradiation, and some chemicals, but also by infection with some bacteria or viruses (36). Rhinovirus activates the SMase for generation of ceramide and forms ceramide-enriched membrane platforms that serve in the infection of

* Corresponding author. Mailing address: Department of Molecular Virology, Research Institute for Microbial Diseases, Osaka University, 3-1 Yamada-oka, Suita, Osaka 565-0871, Japan. Phone: 81-6-6879-8340. Fax: 81-6-6879-8269. E-mail: matsuura@biken.osaka-u.ac.jp.

▽ Published ahead of print on 6 January 2010.

target cells (10). Sindbis virus also activates the SMase and induces apoptosis through a continuous release of ceramide (15). In contrast to these viruses, ceramide inhibits infection with HIV (7) and HCV (48). Ceramide enrichment of the plasma membrane reduces expression of HCV receptor molecules through an ATP-independent internalization and impairs entry of HCV.

Pseudotype and recombinant viruses based on the vesicular stomatitis virus (VSV) bearing foreign viral envelope proteins have been shown to be powerful tools for the investigation of viral entry and the development of vaccines. These systems have been used to study infection with viruses that do not propagate readily (31, 43) or that are difficult to handle due to their high-level pathogenicity for humans (42). In addition, the systems allow us to focus on the investigation of entry mechanisms of particular viral envelope proteins by using control viruses harboring an appropriate protein on identical particles.

In the present study, we generated pseudotype (JEVpv) and recombinant (JEVrv) VSVs bearing the JEV envelope protein in human cell lines and determined the involvement of sphingolipids, especially ceramide, and cholesterol in infection of human cell lines with JEV. Both JEVpv and JEVrv exhibited infection of target cells via pH- and clathrin-dependent endocytosis. Treatment of cells with cholesterol impaired infection with JEVpv and JEVrv, as previously found in JEV infection (20). In contrast, treatment of cells with SMase drastically enhanced infection with both JEVpv and JEVrv and the production of infectious JEVrv particles. These results indicate that ceramide plays crucial roles in the entry and egress of JEV.

MATERIALS AND METHODS

Plasmids and cells. A cDNA clone encoding the PrM and E proteins of the AT31 strain was generated by PCR amplification, cloned into pCAGGS/MCS-PM (43), and designated pCAGC105E (JEV). The plasmid used for construction of JEVrv was pVSVΔG-GFP2.6 (provided by M. A. Whitt, University of Tennessee), which has additional transcription units with multicloning sites (MCS) and green fluorescent protein (GFP) located between the M and L genes. The PrM-E gene, obtained from pCAGC105E (JEV) by digestion with BglII and EcoRI, was cloned into the SmaI site of pVSVΔG-GFP2.6 after blunting, and the construct was designated pΔG-JEV (PrM-E). Huh7, BHK, Vero, and 293T cells were cultured in Dulbecco's modified Eagle's medium (DMEM) (Sigma, St. Louis, MO) containing 10% fetal bovine serum (FBS).

Viruses and chemicals. Wild-type JEV was used as described previously (29). The virus was amplified on Huh7 cells and stored at −80°C. The infectious titer was determined by using a focus-forming assay as described below. Bafilomycin A_1 from *Streptomyces griseus* was purchased from Fluka (Sigma). Chlorpromazine hydrochloride, sphingomyelinase (SMase), phospholipase C from *Bacillus cereus*, methyl-β-cyclodextrin (MβCD), a water-soluble cholesterol, and amitriptyline hydrochloride were obtained from Sigma. C_6-ceramide and sphingomyelin were purchased from Biomol International (Plymouth Meeting, PA). Biotin-ceramide was purchased from Echelon Biosciences Inc. (Salt Lake City, UT).

Reverse genetics of VSV. Recombinant VSVs were generated by a previously described method (43) with minor modifications. Briefly, BHK cells were grown to 90% confluence on 35-mm tissue culture plates and infected with a recombinant vaccinia virus encoding T7 RNA polymerase at a multiplicity of infection (MOI) of 5. After incubation at room temperature for 1 h, the cells were transfected with 4 μg of mixed plasmids encoding each component of VSV proteins (pBS-N/pBS-P/pBS-L/pBS-G, 3:5:1:8) and 2 μg of pΔG-Luci or pΔG-JEV (PrM-E) plasmid using the *Trans*IT-LT1 transfection reagent (Mirus, Madison, WI). After 48 h of incubation, the supernatants were passed through a filter with a pore size of 0.22 μm (Milex-GS; Millipore, Tokyo, Japan) to remove vaccinia virus and inoculated into 293T cells that had been transfected with pCAGVSVG (25) 24 h previously. Recovery of progeny virus was assessed by the appearance of cytopathic effects at 24 to 36 h postinfection. VSV G-complemented (*G) recombinant viruses were stored at −80°C. The infectious titers of the recovered viruses were determined by a plaque assay.

Production and characterization of JEVpv, JEVrv, and JEV. To generate JEVpv, Huh7 cells transiently expressing the PrM and E proteins by the transfection with pCAGC105E using *Trans*IT-LT1 (Mirus) were infected with VSVΔG/Luc-*G, in which the G gene was replaced with the luciferase gene and was pseudotyped with the G protein, at an MOI of 0.1. The virus was adsorbed for 2 h at 37°C and then extensively washed four times with serum-free DMEM. After 24 h of incubation at 37°C with 10% FBS-DMEM, the culture supernatants were centrifuged to remove cell debris and stored at −80°C. To generate JEVrv, Huh7 cells were infected with VSVΔG/JEV-*G at an MOI of 5 for 2 h at 37°C and then extensively washed four times with serum-free DMEM. After 24 h of incubation at 37°C with 10% FBS-DMEM, the culture supernatants were collected and stored at −80°C. Schematic representations of the genome structures and the production of recombinant and pseudotype VSVs are shown in Fig. 1. The purification and concentration of the pseudotype or recombinant viruses were conducted as described previously (43). Purified viruses and infected cell lysates were analyzed by immunoblotting to detect the incorporation of the envelope protein with anti-JEV E mouse polyclonal antibody (E#2-1; unpublished). The infectivities of JEVpv, JEVrv, and JEV were assessed by both luciferase activity and a focus-forming assay, as described below. The relative light unit (RLU) value of luciferase was determined by using the Bright-Glo luciferase assay system (Promega Corporation, Madison, WI), following a protocol provided by the manufacturer. To examine the effects of oligosaccharide modification of the JEV E protein in cells or on the particles, the cell lysates and the purified particles were digested with endoglycosidase H (Endo H) or peptide-N-glycosidase F (PNGase F) (Boehringer Mannheim, Mannheim, Germany), following a protocol provided by the manufacturer, and analyzed by immunoblotting.

Pseudotype VSVs bearing HCVE1E2 (HCVpv), VSVG (VSVpv), and murine leukemia virus envelope (MLVpv) proteins were produced in 293T cells transfected with pCAGc60-p7 (H77), pCAGVSVG, and pFBASALF (provided by T. Miyazawa, Kyoto University), respectively, and used as controls. Recombinant HCV (HCVrv) was also used as a control as described previously (43). To neutralize infection with JEVpv, JEVrv, and JEV, viruses were preincubated with the indicated dilution of anti-JEV E monoclonal antibody (22A1; provided by E. Konishi, Kobe University) for 1 h at 37°C and then inoculated into Huh7 cells. After 1 h of adsorption, the cells were washed three times with DMEM containing 10% FBS, and infectivity was determined after 24 h of incubation at 37°C.

Focus-forming assays. Cells infected with JEV, VSV, JEVrv, or HCVrv after treatment with the indicated reagents were cultured at 37°C with 0.8% methylcellulose in 10% FBS-DMEM for 24 or 48 h and fixed with 4% paraformaldehyde solution for 1 h. Cells were washed once with phosphate-buffered saline (PBS), treated with 0.5% Triton X-100 for 20 min for permeabilization, incubated with mouse monoclonal antibody to JEV (MsX Japanese encephalitis; Chemicon International Inc., Temecula, CA) for JEV or that to VSV N (10G4; provided by M. A. Whitt) for VSV, JEVrv, and HCVrv for 1 h, and stained by using a Vectastain Elite ABC anti-mouse IgG kit with a VIP substrate (Vector Laboratories, Burlingame, CA), following a protocol provided by the manufacturer.

Effects of chemicals on the infectivities of JEVpv, JEVrv, and JEV. To examine the entry pathways of the viruses, cells treated with various concentrations of bafilomycin A_1, chlorpromazine, MβCD, SMase, phospholipase C, or amitriptyline for 1 h at 37°C were inoculated with JEVpv, HCVpv, VSVpv, or MLVpv, and infectivity was determined by luciferase activity as described above. To examine the effects of cholesterol or SMase on the viral particles, purified virions incubated with various concentrations of water-soluble cholesterol or SMase for 1 h at 37°C were inoculated into the target cells. Viruses treated with SMase were ultracentrifuged (43) and resuspended in culture media to deplete any residual amount of SMase, and infectivity was determined by luciferase or focus-forming assay. To examine the effects of ceramide on the infection, 10 mM C_6-ceramide or sphingomyelin dissolved in ethanol was diluted with medium at various concentrations and preincubated with JEVpv, HCVpv, VSVpv, or MLVpv for 1 h at 37°C. After treatment, the viruses were inoculated into Huh7 cells, washed with medium after 1 h of incubation at 37°C, and cultured for 24 h at 37°C, and the residual infectivity was determined by measuring luciferase activity. The effects of C_6-ceramide on the infection of JEV were assessed by following the same protocol, and the residual infectivity was determined by focus-forming assay.

Ceramide binding assay. To examine the interaction of JEV E protein and ceramide, purified viruses were incubated with 500 μl of lysis buffer (20 mM Tris-HCl, pH 7.4, containing 135 mM NaCl and 1% Triton X-100) supplemented

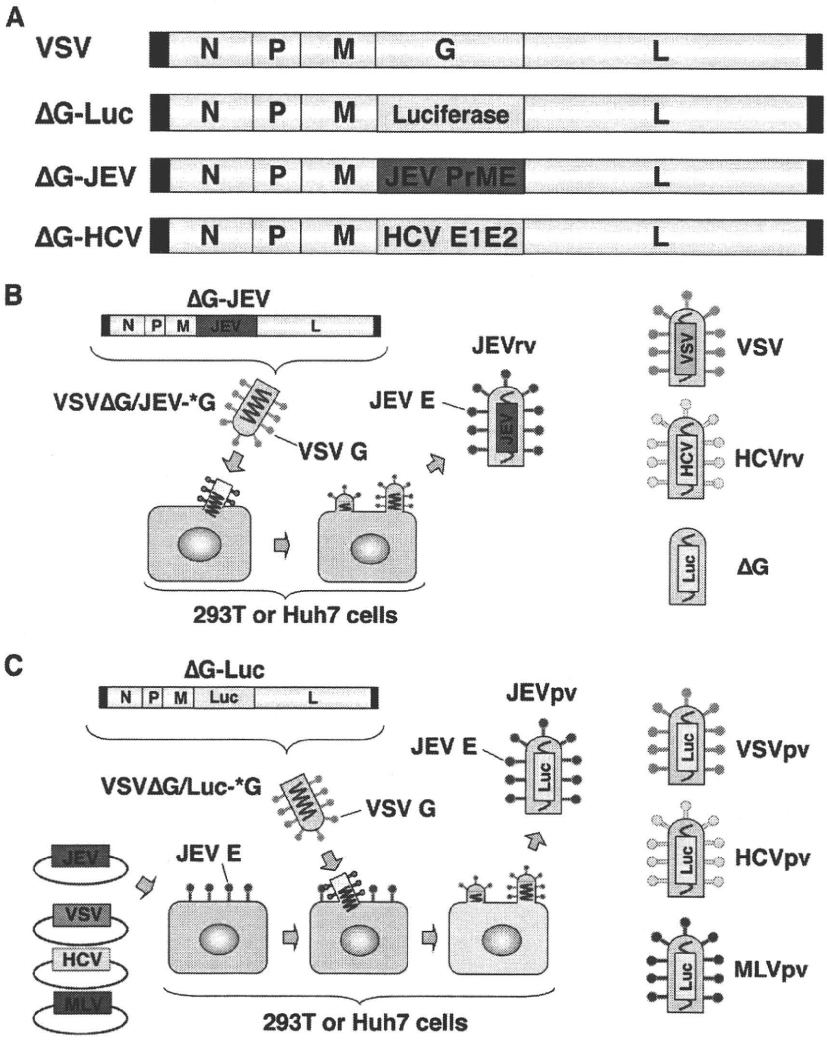

FIG. 1. Schematic representation of the genome structures and production of recombinant and pseudotype VSVs. (A) The luciferase, PrME, and E1E2 genes were inserted into the full-length cDNA clone of VSV in place of the G gene and designated ΔG-Luc, ΔG-JEV, and ΔG-HCV, respectively. (B) Recombinant VSVs, JEVrv, HCVrv, and ΔG, bearing the JEV E protein, HCV E1/E2 proteins, and no envelope, respectively, were generated in 293T or Huh7 cells by infection with the respective recombinant VSV after complementation with VSV G protein (*G). (C) Pseudotype VSVs, JEVpv, VSVpv, HCVpv, and MLVpv, were generated by infection with VSVΔG/Luc-*G in 293T or Huh7 cells transiently expressing the respective foreign protein.

with protease inhibitor cocktail (Roche, Indianapolis, IN) and 10 μl of 1-mg/ml biotin-ceramide in dimethyl sulfoxide (DMSO) for 1 h at 37°C, and then 20 μl of streptavidin-Sepharose 4B (Zymed, Invitrogen, Carlsbad, CA) was added and the solution was kept at 4°C for 4 h. After washing with the lysis buffer three times, the pellets were analyzed by immunoblotting with anti-JEV E polyclonal antibody (E#2-1).

RESULTS

Construction and characterization of recombinant and pseudotype VSVs. Recombinant VSVs were propagated in Huh7 cells by infection with VSVG-complemented (*G) recombinant VSVs possessing foreign genes of either JEV PrM/E, HCV E1/E2, or luciferase in place of the VSV G gene, as shown in Fig. 1A and B. The pseudotype VSVs, JEVpv, VSVpv, HCVpv, and MLVpv, were generated by infection with VSVΔG/Luc-*G in 293T or Huh7 cells transiently expressing the respective foreign protein (Fig. 1C).

To examine the properties of the JEV E proteins incorporated into JEV, JEVrv, and JEVpv particles, the E proteins expressed in Huh7 cells and incorporated into the viral particles were digested with Endo H or PNGase F and examined by immunoblotting (Fig. 2A). Although E proteins in the lysates of cells infected with JEV, JEVrv, or JEVpv were sensitive to both Endo H and PNGase F treatments, those incorporated into the viral particles were resistant to Endo H, suggesting that both JEVrv and JEVpv particles selectively incorporate the matured E proteins modified to the complex- or hybrid-type glycans as seen in the authentic JEV particles. Next, to examine the infectivity of JEVrv and JEVpv for the target cells, HCVpv, MLVpv, VSVpv, VSV, HCVrv, and ΔG were prepared as controls (Fig. 2B). Both JEVpv and JEVrv were infectious for Huh7, BHK, and Vero cells, whereas HCVpv and HCVrv were infectious for Huh7 cells but not for BHK

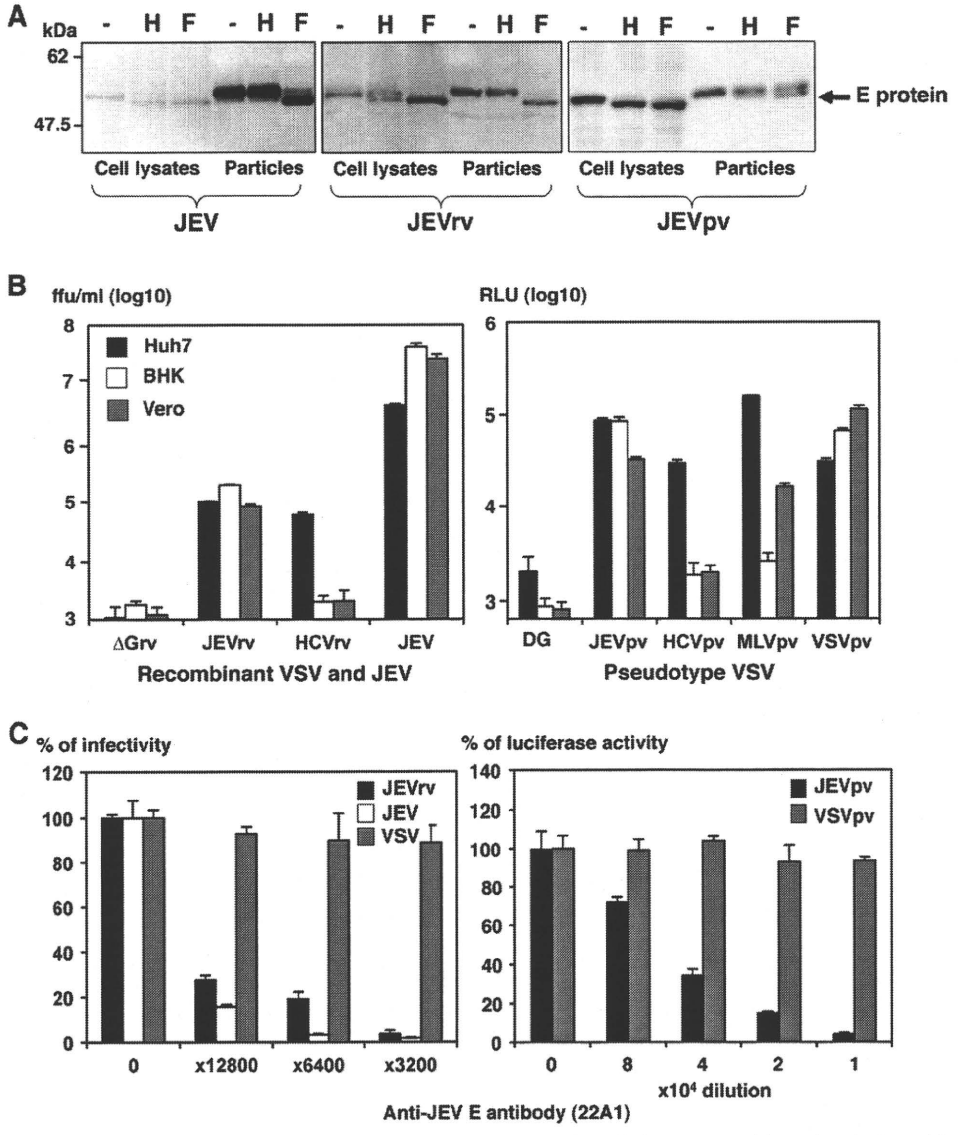

FIG. 2. Characterization of JEVrv and JEVpv. (A) JEV E proteins expressed in cells incorporated into the viral particles were treated with endoglycosidase H (H) or peptide-N-glycosidase F (F) and examined by immunoblotting using anti-E polyclonal antibody. "-" indicates an untreated sample. (B) Infectivities of recombinant viruses (left panel) and pseudotype viruses (right panel) were determined in Huh7, BHK, and Vero cells by a focus-forming assay and measurement of luciferase activity (RLU), respectively. VSV without envelope (ΔG) was used as a negative control. ffu, focus-forming units. (C) Neutralization of JEVrv (left panel) or JEVpv (right panel) infection by anti-E polyclonal antibody. Viruses were incubated with the indicated dilution of antibody for 1 h at room temperature and inoculated into Huh7 cells. Residual infectivities are expressed as percentages. VSV and VSVpv were used as controls. The results shown are from three independent assays, with error bars representing standard deviations.

and Vero cells, as previously reported (1). Although JEVpv and JEVrv generated in 293T cells were also infectious, these viruses were slightly more infective when generated in Huh7 cells, even though the efficiency of transfection of the expression plasmids into 293T cells was higher than that of transfection into Huh7 cells (data not shown). To determine the specificity of infection of JEVpv, JEVrv, and JEV, a neutralization assay was performed by using anti-E antibody (22A1). The infectivities of JEVpv and JEVrv but not of VSVpv and VSV for Huh7 cells were clearly inhibited by anti-E antibody in a dose-dependent manner (Fig. 2C). These results suggest that the JEVrv and JEVpv generated in this study had characteristics comparable to those of authentic JEV.

Entry pathways of JEVpv. Previous studies showed that JEV infection was inhibited by treatment with inhibitors of vacuolar acidification, such as ammonium chloride, concanamycin A, and bafilomycin A_1, suggesting that JEV enters target cells via pH-dependent endocytosis (30). Other flaviviruses, including WNV, DENV, and HCV, exhibit similar entry mechanisms (18, 45). To compare the entry pathway of JEV with those of other viruses, Huh7 cells were pretreated with various concentrations of bafilomycin A_1 and then the cells were inoculated

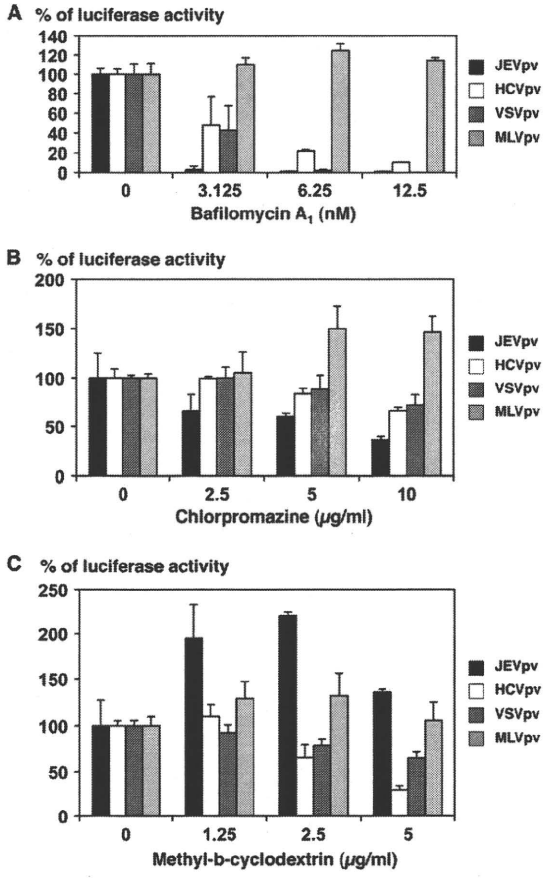

FIG. 3. Entry pathways of the pseudotype VSVs. Huh7 cells were pretreated with various concentrations of bafilomycin A_1 (A), chlorpromazine (B), or methyl-β-cyclodextrin (C) for 1 h and inoculated with the pseudotype viruses, JEVpv, HCVpv, VSVpv, and MLVpv. Luciferase activities were determined at 24 h postinfection. The results shown are from three independent assays, with error bars representing standard deviations.

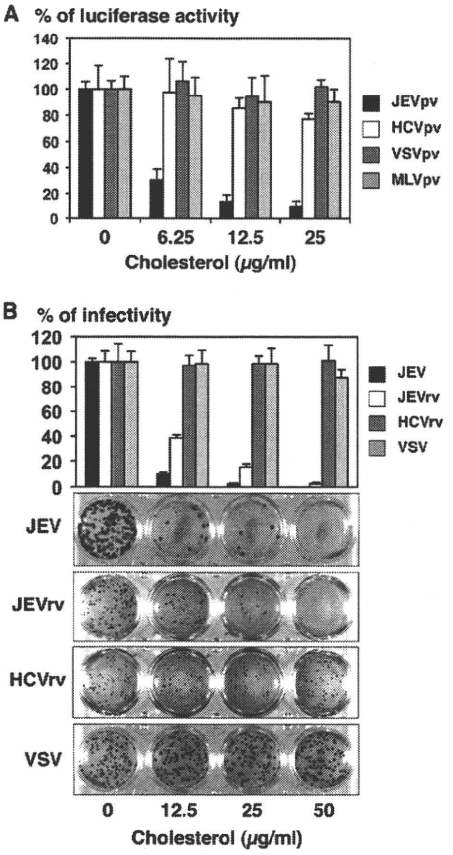

FIG. 4. Effects of cholesterol on infection with recombinant and pseudotype VSVs. (A) The pseudotype viruses were incubated with various concentrations of cholesterol for 1 h at room temperature and inoculated into Huh7 cells, and luciferase activities were determined at 24 h postinfection. (B) JEV, JEVrv, HCVrv, and VSV were incubated with various concentrations of cholesterol for 1 h at room temperature and inoculated into Huh7 cells, and residual infectivities were determined by focus-forming assay in a culture medium containing 1% methylcellulose at 48 h postinfection for JEV, JEVrv, and HCVrv and at 24 h postinfection for VSV. Foci of infected cells were detected by immunohistochemical staining (lower panel). The rate of focus formation of the viruses was analyzed by counting foci. The results shown are from three independent assays, with error bars representing standard deviations.

with JEVpv, HCVpv, VSVpv, and MLVpv (Fig. 3A). As expected, bafilomycin A_1 treatment did not affect the infectivity of MLVpv-bearing envelope proteins of MLV, which enters cells through a pH-independent direct fusion of the viral membrane and plasma membrane. In contrast, infections with HCVpv and VSVpv, which enter cells through pH-dependent endocytosis, were inhibited by treatment with bafilomycin A_1 in a dose-dependent manner. Similarly, infection with JEVpv was clearly inhibited by treatment with bafilomycin A_1 in a dose-dependent manner, suggesting that JEVpv enters cells through pH-dependent endocytosis, as seen in JEV infection.

To further examine the entry pathway of JEVpv, Huh7 cells were pretreated with various concentrations of chlorpromazine, an inhibitor of clathrin-mediated endocytosis, or MβCD, an inhibitor of caveolar/raft-mediated endocytosis, and infected with the pseudotype viruses. The infectivity of MLVpv was not affected by the treatment with either chlorpromazine or MβCD, as we expected. Treatment of cells with chlorpromazine slightly reduced the infectivity of JEVpv, HCVpv, and VSVpv in a dose-dependent manner (Fig. 3B), whereas treatment of cells with MβCD reduced the infectivity of HCVpv and VSVpv but increased the infectivity of JEVpv (Fig. 3C). These results suggest that JEVpv enters cells via clathrin-mediated endocytosis, as previously reported for infection with JEV (30), and that caveola/raft plays a different role in the entry of JEV than in the entry of HCV and VSV.

Effects of cholesterol on the entry and egress of JEV. Recently it was shown that entry of flaviviruses, including JEV and DENV, was drastically inhibited by treatment of the particles with cholesterol (20). To examine the effect of cholesterol on entry of JEV, the pseudotype viruses were inoculated into Huh7 cells after treatment with various concentrations of cholesterol. The infectivity of JEVpv but not that of HCVpv, VSVpv, or MLVpv was severely impaired by treatment with cholesterol in a dose-dependent manner (Fig. 4A). Next, to examine the effect of cholesterol on the propagation of JEV, the recombinant viruses were inoculated into Huh7 cells after

treatment with various concentrations of cholesterol. Infectivities of JEV and JEVrv but not those of VSV and HCVrv were inhibited by the treatment with cholesterol (Fig. 4B, upper panel). Suppression of the propagation of JEV and JEVrv was further confirmed by a focus-forming assay (Fig. 4B, lower panels). These results confirmed that JEV entry was suppressed by cholesterol, as previously reported (20), and raise the possibility that cholesterol participates not only in entry via the E protein but also in the assembly of the E protein. These data also support the notion that JEVpv and JEVrv are comparable to JEV in terms of the properties of the E protein involved in the entry and egress processes.

Effects of SMase on infection with JEVpv, JEVrv, and JEV. Because infection with enveloped viruses was initiated by the interaction of viral and host membrane lipids, we next examined the involvement of membrane lipids in the entry of JEV. Sphingolipid is a major component of eukaryotic lipid membranes, and sphingomyelin is one of the most abundant sphingolipids, with a wide presence across the cell membrane. SMase is known to cleave sphingomyelin, yielding phosphorylcholine and ceramide. To examine the effect of SMase on viral infection, cells were infected with viruses after treatment with various concentrations of SMase, and the infectivities of the viruses were assessed by the luciferase or focus-forming assay. Infection with JEVpv was drastically enhanced by SMase treatment of Huh7 cells, whereas such treatment exhibited no effect on infection with VSVpv and MLVpv and suppressed HCVpv infection (Fig. 5A). The enhancement of JEVpv infection by SMase treatment was also observed in other cell lines, including BHK and Vero cells (data not shown). Although the effect was not as evident as in JEVpv infection, SMase treatment exhibited a slight but substantial enhancement of the infectivity of JEV and JEVrv in Huh7 cells, in contrast to having no effect on VSV infection and a suppressive effect on HCVrv infection (Fig. 5B). The difference in the magnitude of enhancement of infectivity by treatment with SMase between infection with JEVpv and that with JEV or JEVrv might be attributable to the difference in the viral systems based on pseudotype (JEVpv) and replication-competent (JEV and JEVrv) viruses, which allow single and multiple rounds of infection, respectively. The effects of SMase may be more critical for the entry step than for other, later steps of infection. Suppression of HCVpv and HCVrv infection by treatment with SMase was consistent with previously reported data on infection of HCV-pseudotyped retroviral particles (HCVpp) and JFH1 virus (48).

Next, we examined the effect of SMase on the viral particles. Treatment of pseudotype particles of JEVpv, VSVpv, and MLVpv with various concentrations of SMase had no significant effect on their infectivity for Huh7 cells (Fig. 5C), whereas the infectivity of HCVpv particles was impaired by the treatment in a dose-dependent manner, as reported previously (1), suggesting that SMase treatment enhances the infectivity of JEVpv by modifying the molecules on target cells rather than the molecules on viral particles. To further determine the involvement of SMase in infection of JEVpv, cells were pretreated with various concentrations of amitriptyline, an inhibitor of acid SMase. The infectivity of JEVpv but not that of other viruses was decreased by the treatment with amitriptyline in a dose-dependent manner (Fig. 5D). A similar effect was observed with treatment with another SMase inhibitor, imipramine (data not shown). Collectively, these results suggest that entry of JEV into the target cells is enhanced by SMase treatment, which modifies the cell surface sphingolipids into a more competent state for interaction with the JEV envelope protein, thereby enabling its entry.

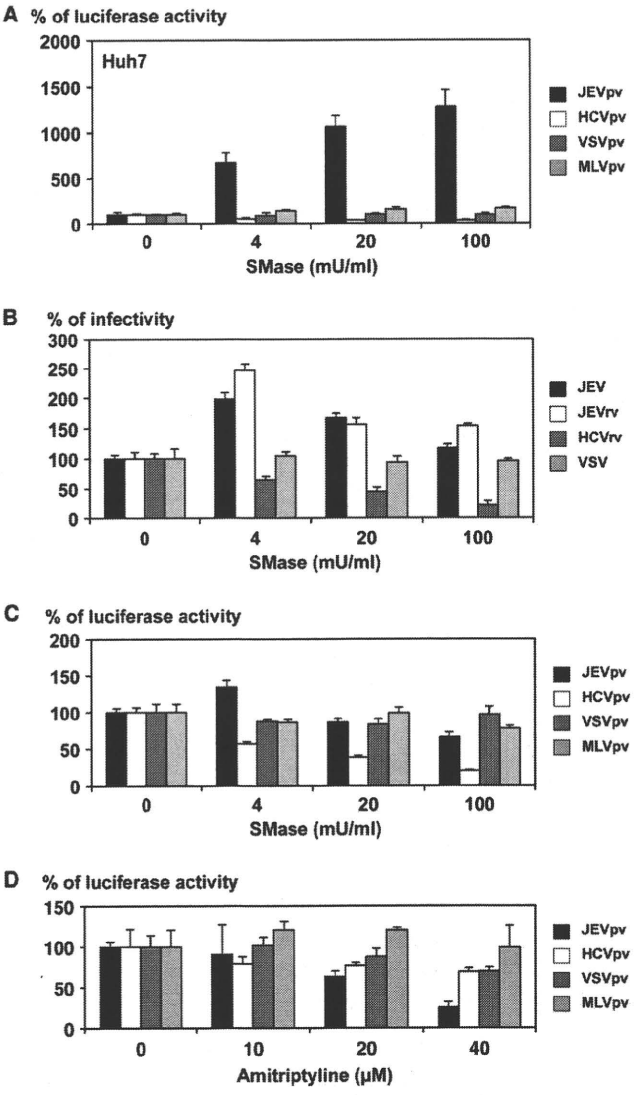

FIG. 5. Effects of SMase and amitriptyline treatment of cells on infection with pseudotype and recombinant VSVs. Huh7 cells were pretreated with various concentrations of SMase for 1 h, and then pseudotype viruses (A) or recombinant viruses (B) were inoculated. The infectivities were determined by luciferase activity measurement or focus-forming assay, and changes in infectivities are expressed as percentages. (C) The purified pseudotype particles were treated with various concentrations of SMase for 1 h and inoculated into Huh7 cells after removal of SMase by ultracentrifugation. Infectivities were determined at 24 h postinfection by measuring luciferase activity, and changes in infectivities are expressed as percentages. (D) Huh7 cells were pretreated with various concentrations of amitriptyline, an inhibitor for the acid SMase, for 1 h, and then pseudotype viruses were inoculated. Infectivities were determined at 24 h postinfection by measuring luciferase activity, and changes in infectivities are expressed as percentages. The results shown are from three independent assays, with error bars representing standard deviations.

Effects of SMase on propagation of JEVrv and JEV. We next examined the effects of SMase on the propagation of JEV. Recombinant VSV is capable of replicating by using the VSV genome and producing infectious particles bearing a foreign envelope protein encoded in place of the original G protein, and thus, it is feasible to assess the efficiency of not only entry but also egress of the recombinant viruses possessing foreign envelope genes of different origins, irrespective of their replication efficiency within the target cells. To examine the effects of SMase on viral propagation, cells were treated with various concentrations of the enzyme, inoculated with the recombinant viruses, and then cultured for up to 48 h in the presence of SMase. Production of JEVrv was dramatically enhanced by cultivation in the presence of SMase, in contrast to the suppression of HCVrv propagation (Fig. 6A). Although the effect of SMase treatment on the production of JEV was not as great as that seen in JEVrv propagation, treatment with SMase resulted in a substantial enhancement of JEV but not of VSV propagation (Fig. 6B). These results suggest that SMase treatment induces robust propagation of JEVrv mainly through enhancement of the entry step although also partly through enhancement of the egress step.

Involvement of ceramide in infection with JEV. Because treatment of cells with SMase induces production of ceramide, we next examined the effect of ceramide on the infectivity of the viruses. Treatment of the pseudotype particles with C_6-ceramide inhibited the infectivity of JEVpv for Huh7 cells in a dose-dependent manner, whereas no clear reduction of infectivity was observed with treatment of HCVpv, VSVpv, and MLVpv with ceramide (Fig. 7A). In contrast, treatment of the pseudotype particles with sphingomyelin, which is a substrate for SMase and is catalyzed into ceramide, did not affect the infectivity of the viruses, suggesting that the enhancement of infectivity of JEVpv by treatment with SMase was due to the generation of ceramide. Propagation of JEV but not of VSV was also suppressed by treatment of the viral particles with C_6-ceramide in a dose-dependent manner (Fig. 7B). Finally, to confirm the interaction of the JEV E protein with ceramide, purified JEV and JEVrv particles were incubated with biotin-ceramide and streptavidin-Sepharose 4B and examined by pull-down assay (Fig. 7C). The E proteins of both JEV and JEVrv were precipitated with the ceramide beads. These results indicate that the interaction of the JEV E protein with ceramide plays a crucial role in the entry of JEV.

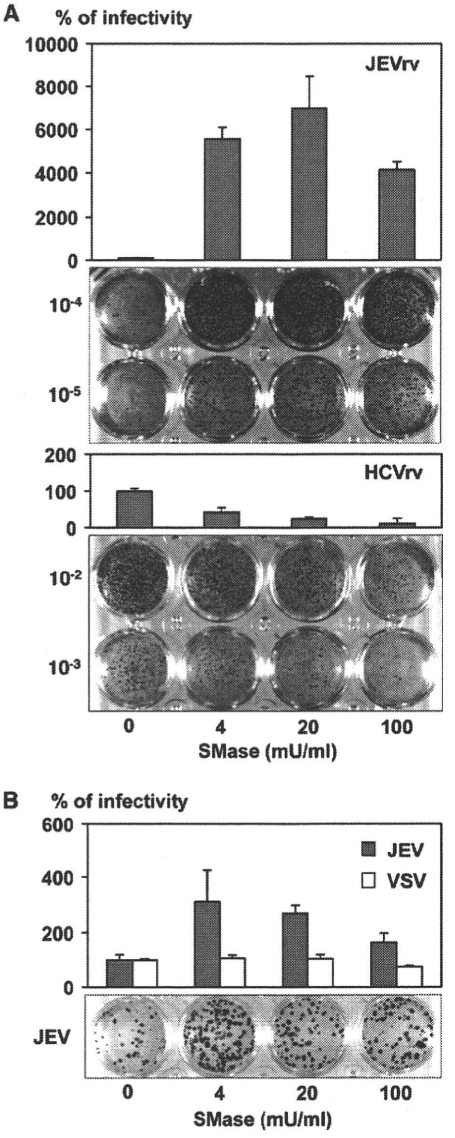

FIG. 6. Effects of SMase on the propagation of JEVrv and JEV. Huh7 cells were pretreated with various concentrations of SMase for 1 h and inoculated with JEVrv or HCVrv (A) or JEV or VSV (B), and infectivities were determined by focus-forming assay in a culture medium containing 1% methylcellulose at 48 h after infection with JEVrv, HCVrv, and JEV and at 24 h after infection with VSV. Titers were determined by counts of foci detected by immunohistochemical staining (lower panels). The results shown are from three independent assays, with error bars representing standard deviations.

DISCUSSION

Ceramide has been shown to play a crucial role in various cell signaling pathways through the clustering and activation of the receptor molecules in lipid rafts. Although the generation of ceramide inhibits the infectivity of HIV and HCV by the rearrangement of the entry receptor molecules (7, 48), rhinovirus and Sindbis virus generate ceramide by activating SMase for their entry and cell survival, respectively (10, 15). In this study, we demonstrated for the first time that ceramide plays crucial roles not only in the entry pathway of JEV but also in the egress through a direct interaction with the E envelope proteins.

To examine the roles of the E protein in the infectivity of JEV, we employed pseudotype and recombinant VSVs bearing JEV envelope proteins as surrogate systems in addition to authentic JEV. VSV assembles and buds from the plasma membrane, and therefore the surrogate viruses bearing the foreign envelope proteins being expressed on the plasma membrane exhibited more-efficient incorporation of the envelope proteins. Although the E protein of JEV, as well as that of other flaviviruses, including HCV, is mainly retained on the endoplasmic reticulum (ER) membrane, the E protein was incorporated into JEVpv and JEVrv particles and exhibited infectivity comparable to that of authentic JEV. Further studies are needed to clarify the mechanisms of incorporation of